TR-40
1971

Dynamic Simulation of Unsteady Flow of Water in Unsaturated Soils and its Application to Subirrigation System Design

E.A. Hiler
S.I. Bhuiyan

Texas Water Resources Institute

Texas A&M University

RESEARCH PROJECT INTERIM REPORT

Project Number B-080-TEX

July 1, 1970-June 30, 1972

Agreement Number

14-31-0001-3338

DYNAMIC SIMULATION OF UNSTEADY FLOW OF WATER IN UNSATURATED SOILS AND ITS APPLICATION TO SUBIRRIGATION SYSTEM DESIGN

E. A. Hiler
S. I. Bhuiyan

The work upon which this publication is based was supported in part by funds provided by the United States Department of the Interior, Office of Water Resources Research, as authorized under the Water Resources Research Act of 1964.

Technical Report No. 40
Texas Water Resources Institute
Texas A&M University
November 1971

ABSTRACT

Unsteady vertical flow of water in unsaturated soils was simulated utilizing S/360 CSMP (Continuous System Modeling Program), a recently developed language specially designed for digital simulation of transient phenomena that can be represented by differential equations. The principles of conservation of mass and of Darcy's law, which lead to the derivation of the unsaturated flow equation, were directly applied to specify the flow system. The boundary conditions described a no-flow situation across the top surface and an impermeable layer across the bottom of the soil mass considered. The initial condition specified a uniform pressure potential, corresponding to a water content uniform with depth.

Two computer programs were developed. One simulated vertical unsteady infiltration through the surface into a homogeneous unsaturated soil. Simulation results were obtained for three different soils--Yolo light clay, Adelanto loam, and Pachappa loam. The results for Yolo light clay compared favorably with the available numerical solutions of Philip for the same soil and for identical boundary and initial conditions. The solutions for the other two soils demonstrated the workability of the model for soils having different hydraulic characteristics.

The other computer model simulated unsteady vertical flow of water in an unsaturated homogeneous soil during infiltration from a buried source and through the following drying period, in a sequence. The consumption of water by plant roots, considered to be a nonlinear function of the time of day, was taken into account. The consumption rate at

any given time was assumed to be distributed in a linearly decreasing manner with depth of the root zone. The model has the capacity to consider the source at any desired level.

Simulation data for buried sources were obtained for Yolo light clay, using a soil depth as well as a root depth of 60 cm, in two sets. The first set had an initial uniform water content of 0.2375 (cm^3/cm^3), whereas 0.32 (cm^3/cm^3) was the value for the second set. A daily root consumption of 0.635 cm was used. In each set, three different depths of the source, i.e., 10, 20, and 30 cm, were used. For each source location, simulation results were obtained for varying durations of the irrigation and drying cycle which were controlled by a chosen water content value at a specified point in the soil mass. The whole system, thus, worked like an automated subirrigation installation.

The water content profiles with time were plotted for each simulation run. The patterns of water distribution with time for each source location were analyzed in light of two important criteria: (i) adequacy of the supply of water with respect to the need at different parts of the root zone, and (ii) overall irrigation efficiency. Two new concepts, availability coefficient and proportionality coefficient, which help evaluate the effectiveness of vertical water distribution in a subirrigation system, were defined and illustrated.

For the assumed distribution of the root consumption with time and depth, the 10-cm depth source provided better distribution of water with time and space compared to the 20-cm and 30-cm source locations. Irrigation from zero depth, as in the case of trickle irrigation, appeared to be the best system for the given conditions.

The S/360 CSMP language proved to be efficient in simulating the transient water flow phenomena in unsaturated soils. The principal advantage of the numerical procedure followed was in its complete generality and the ease with which numerical data on the hydraulic characteristics of the soil may be used without arbitrary assumptions and function fitting procedures. The models developed are capable of considering diverse boundary and initial conditions.

TABLE OF CONTENTS

LIST OF TABLES

LIST OF FIGURES

LIST OF FIGURES (continued)

LIST OF FIGURES (continued)

LIST OF FIGURES (continued)

CHAPTER I

INTRODUCTION

The tremendous increase in the demand for irrigation water over the past years has put enormous pressures on the water resources of the nation. In the High Plains of Texas, where ground water supplies are declining every day, the cost of irrigation water is already at a premium. It is estimated that a serious shortage of ground water in that area will occur by 1990 if the present rate of depletion is continued. As such, improvements over the existing methods or new techniques in irrigation aimed at curtailing the water losses are in greater need today than ever before. Subirrigation, the technique of applying the water beneath the soil surface through multiorificed or porous synthetic pipes, shows great promise in this respect.

One of the primary benefits resulting from the use of subirrigation is the substantial increase in the irrigation efficiency compared to the conventional methods. Since the water is applied in the root zone of the plant where it is actually consumed, all the facets that constitute irrigation efficiency, i.e., water-application efficiency, water-use efficiency, etc., can be maintained at a high degree of efficiency. Prevention of surface wetting results in considerable curtailment of water loss by surface evaporation. A 20 to 40 percent

savings in irrigation water could be expected in cotton production in Texas with subirrigation when compared to a well designed surface system (Zetzsche and Newman, 1966).

A mathematical model capable of predicting the movement of water in unsaturated soils during irrigation from a buried source and redistribution is essential for development of a subirrigation system design method. This work was specifically aimed toward achieving that goal. The objectives were:

1. To develop a dynamic computer model that would describe the transient flow of water in an unsaturated soil during and after irrigation from a buried source. The model should take into account the effects of gravity and the consumption of water by plant roots as a dynamic process.

2. To characterize criteria for a subirrigation system design and to develop an approach utilizing the model for determining the optimum depth of the subirrigation source.

3. To examine possibilities of utilizing the computer model for scheduling of subirrigation.

CHAPTER II

REVIEW OF LITERATURE

The theory of flow of water in unsaturated soils is the theoretical basis for the design of subirrigation systems. By use of the equation of continuity and Darcy's law, Klute (1951) derived explicitly the equation for flow of water in unsaturated media.

The continuity equation for flow through a homogeneous soil, as shown in Figure 1, is

$$\frac{\delta(\rho\theta)}{\delta t} = -\left[\frac{\delta(\rho v_x)}{\delta x} + \frac{\delta(\rho v_y)}{\delta y} + \frac{\delta(\rho v_z)}{\delta z}\right] , \qquad (1)$$

where ρ is the fluid density, θ is the volumetric water content, v is the volume flux in the direction of flow, and t is the time.

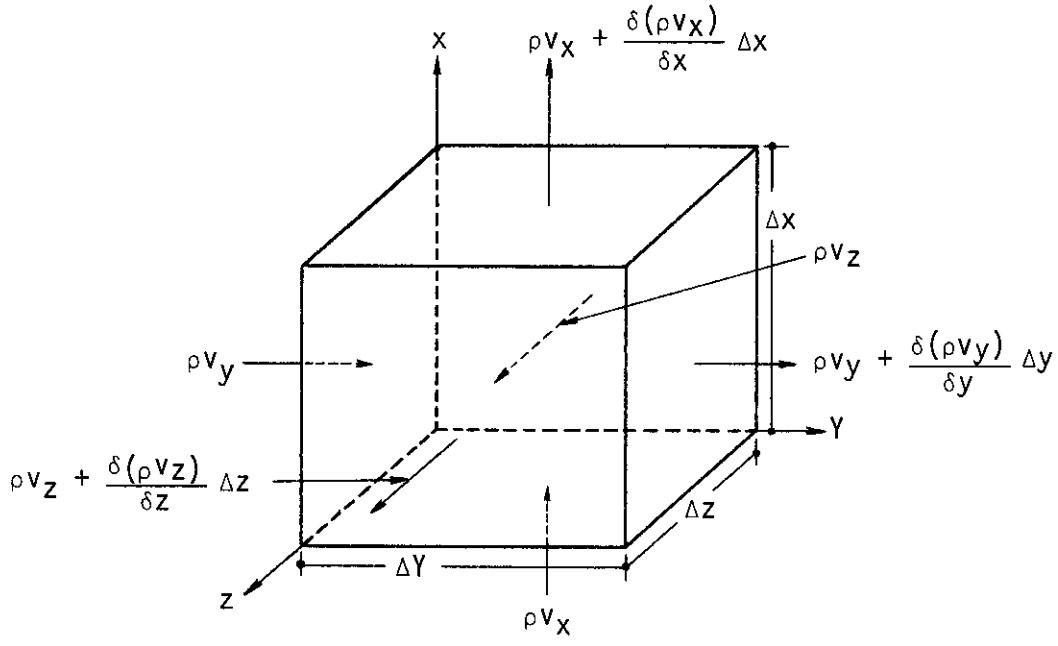

Figure 1 Infinitesimal parallelopiped of soil

Assuming that the volume flux is given by an equation similar to Darcy's law for saturated flow, we have

$$v_x = -K \frac{\delta \phi}{\delta x} ,$$

$$v_y = -K \frac{\delta \phi}{\delta y} , \text{ and} \tag{2}$$

$$v_z = -K \frac{\delta \phi}{\delta z} ,$$

where K is the hydraulic conductivity and ϕ is the hydraulic potential. Substitution of equation (2) into equation (1) yields

$$\frac{\delta(\rho\theta)}{\delta t} = \frac{\delta}{\delta x}(\rho K \frac{\delta \phi}{\delta x}) + \frac{\delta}{\delta y}(\rho K \frac{\delta \phi}{\delta y}) + \frac{\delta}{\delta z}(\rho K \frac{\delta \phi}{\delta z}) . \tag{3}$$

Assuming a constant fluid density, equation (3) can be written in vector form as

$$\frac{\delta \theta}{\delta t} = \nabla \cdot (K \nabla \phi). \tag{4}$$

If the hydraulic potential is considered as the sum of the pressure potential, h, and the gravitional potential, x (positive upward), i.e., if

$$\phi = h + x, \tag{5}$$

and if both h and K are regarded as single-valued functions of θ, equation (4) becomes

$$\frac{\delta \theta}{\delta t} = \nabla \cdot (K \nabla h) + \frac{\delta K}{\delta x} . \tag{6}$$

Equation (4) is the general differential equation for the flow of water through an unsaturated homogeneous porous medium. Equation (6) incorporates the concepts of pressure potential and gravitational potential.

In view of the nature of the differential equation (4) and the nonlinear relations between parameters, most efforts have concentrated on seeking numerical rather than analytical solution of the problem. Pioneering work in this area was done by Philip (1957a, 1969) who developed a numerical solution technique for infiltration into a semi-infinite, homogeneous, one-dimensional soil with uniform initial water content. His solution has the form of a power series in $t^{1/2}$:

$$x = \nu t^{1/2} + \chi t + \psi t^{3/2} + \cdots + f_m(\theta)\, t^{m/2} + \cdots \quad , \tag{7}$$

in which x is the vertical ordinate and the coefficients ν, χ, ψ, ... $f_m(\theta)$ are functions of θ and are the solutions of a series of ordinary differential equations which can be solved by numerical methods (1957a). Philip also established the effect of initial water content and water depth over the soil surface in vertical, one-dimensional infiltration (1957b, 1958). Wang (1963) developed a numerical method for one-dimensional infiltration and her results showed good agreement with those of Philip.

Whisler and Klute (1965) developed a numerical solution for unsteady flow of water in a vertical soil column drained from saturation to equilibrium under gravity with a water table. They used the relaxation technique to solve the pressure head form of equation (6). Whisler and Watson (1968) presented a numerical analysis of the one-dimensional gravity drainage problem using the pressure head form of the differential equation of flow and utilizing a digital computer.

Singh and Franzini (1967) obtained a solution of the two-dimensional diffusion equation for unsteady and unsaturated flow from a cylindrical source of finite radius. Neglecting gravity, they transformed equation (6) into an ordinary differential equation which was solved by a numerical technique. Their procedure was, however, proven to be incorrect by Philip (1968). An approximate solution to the flow from a spherical source with water content dependent diffusivity was obtained by Singh (1970) by the method of weighted residuals.

Shih and Kriz (1969) developed a mathematical solution for unsaturated unsteady radial flow of water in a homogeneous soil surrounding a long infinitely permeable pipe that supplied water under pressure. Their solution considered the effect of gravity. However, application of the solution requires a mean value of the soil-water diffusivity, a concept first introduced by Gardner (1962). This concept is unrealistic because, in unsteady unsaturated flow, the soil-water diffusivity is a time variant parameter.

In a dynamic system where irrigation water is applied to meet transpirational demand of crops, water uptake by plant roots both during and after irrigation is an important part of the whole system. High efficiency in the use of irrigation water requires a minimum of infiltration below the root zone. Knowledge of rooting depth and root activity with depth are therefore important in the design of irrigation systems and to the determination of the proper time and amount of application. Hall et al. (1953) and Hommes and Bartz

(1963) indicated that root uptake decreased rapidly with depth for corn, cotton, and peanuts throughout the growing season. Nakayama and Van Bavel (1963) reported that approximately 90 percent of the water uptake by sorghum occurred from the upper 60 percent of the root zone in all of various irrigation treatments. A general "rule of thumb" frequently used is that 40, 30, 20, and 10 percent of the total transpiration requirement is supplied respectively from each successively deeper one-quarter of the root zone (Danielson, 1967).

The root activity with depth is not a constant factor throughout the entire growing season. Continued development of root branches and their elongation through the soil make the root activity with depth a changing function with time. De Backer and Boersma (1968) developed the concept of "root exploration rate" which is defined as the time rate of change of the depth of maximum root activity. They developed a method of determining the advance of the depth of maximum root activity during the water depletion cycle. They concluded that, combining the water availability coefficient and the porosity of the soil with the root exploration rate, it is possible to predict the rate of water utilization by the plants.

For an accurate evaluation of the actual flow process during and following irrigation, solution of equation (6) having the root uptake function incorporated, is necessary. Whisler et al. (1968) applied numerical analysis to the steady-state flow equation for evapotranspiration from a vertical soil column. The water uptake by the plant roots was incorporated into the flow equation as a constant

negative source term. The final differential equation was expressed as

$$\frac{\delta}{\delta z}\left(K(h)\frac{\delta h}{\delta z}\right) + \frac{\delta K(h)}{\delta z} + S = 0, \qquad (8)$$

where z is the vertical direction and S is the source term. No analogous study has been reported for the unsteady unsaturated flow system.

The dynamic simulation language S/360 CSMP (Continuous System Modeling Program) is a recently developed computer language (IBM, 1967) for analyzing transient phenomena. A problem is defined by a differential equation, or a set of differential equations, with known boundary and initial conditions. Curry (1969) used S/1130 CSMP, an earlier version of S/360, for the dynamic modeling of plant growth. Wierenga and De Wit (1970) utilized S/360 CSMP in simulating transfer of heat in soils. A comprehensive attempt to model plant growth in S/360 CSMP was reported by De Wit et al. (1970) which demonstrated the power of the method for dealing with complex biological systems. Lambert (1971) illustrated the use of CSMP in several agricultural engineering problems.

The preceding review of literature may be summarized by the following general statements:

1. The theory of transient flow of water in unsaturated soils is too complicated to be accurately solved analytically. As a result, researchers have resorted to numerical techniques for solutions. With the advent in recent years of high speed digital computers,

interest in this area has grown considerably.

2. No solution technique is presently available that can yield a usable solution to the problem of unsteady flow of water from subsurface sources while taking into account the effect of gravity as well as the plant root consumption. These considerations are important in subirrigation design.

3. Plant root activity is a dynamic rather than a static characteristic of the plant. It varies with the depth in the soil as well as the time of the day. Also, the pattern of root activity changes with the age of the plant. These are considerations important for accurate accounting of the unsteady flow of water in an unsaturated soil.

4. S/360 CSMP is a computer language designed to simulate phenomena that are changing with time. Its power in dealing with transient systems has been demonstrated. In view of the dynamic nature of the unsteady flow process in an unsaturated soil, this method seems to offer excellent possibilities of producing a useful solution.

CHAPTER III

THE PROBLEM AND ITS SIMULATION

The Problem Statement

The problem is the description of unsteady vertical flow of water in an unsaturated homogeneous soil during and after irrigation from a subsurface source. The effect of gravity as well as the consumption of water by plant roots are to be taken into account. The root consumption is assumed to be a linear function with depth having the maximum value at the surface and gradually decreasing with depth. The consumption rate is a nonlinear function of the time of day and is proportional to the potential evapotranspiration for a day which is assumed to be representative for the growing season.

The following are the boundary and initial conditions considered in this study:

1. There is no flow across the top and bottom boundaries of the soil mass.

2. The soil has a uniform initial pressure potential, corresponding to a water content uniform with depth.

The CSMP Simulation

Two computer programs were developed in the course of this study. The first one simulated the vertical unsteady infiltration

through the surface into a homogeneous unsaturated soil. The second program was used to simulate transient flow of water during infiltration from a buried source and redistribution through the drying circle in a homogeneous unsaturated soil. In this program, the consumption of water by plant roots was taken into account.

The CSMP simulations will be discussed in this section under three subheads: "General Technique," "Infiltration through the Surface," and "Infiltration from Buried Sources and Redistribution." The "General Technique" section will deal mainly with the CSMP modeling method. The computer program for infiltration from buried sources and redistribution will be presented in this section for better understanding of the terminology used to describe the CSMP simulation approach. In the other two sections, the respective details of input data used will be discussed.

General Technique

The simulation model developed to describe unsteady flow of water in unsaturated soils is not restricted to the aforementioned boundary and initial conditions. It is general in form and adaptable equally well to other boundary and initial conditions.

The approach taken in developing the model is fundamentally different from previous methods. Most other approaches, as exemplified by Whisler and Klute (1965), developed a difference equation equivalent to the differential equation (6) which was solved by numerical techniques. But in this model, the basic concepts of

conservation of mass and of Darcy's law, which lead to the derivation of the unsaturated flow equation, were directly applied to specify the flow system.

The modeling concept consisted primarily of dividing the soil vertically into a large number of uniformly thin layers. The hydraulic properties of the soil (conductivity vs. water content; pressure potential vs. water content) being known, the initial hydraulic conductivity (COND), pressure potential (PRPOT), and water content (ICON) values were assigned to the center of each layer. The hydraulic potential in a given layer was always the sum of the pressure potential and gravitational potential (X). The latter was defined as zero at the soil surface. The average hydraulic conductivity (KOND) across a boundary of a layer was calculated by the method of averaging the hydraulic conductivities (COND) of the layers above and below that boundary. The flow rate (FLOWIN) across a given boundary for time $t+\Delta t$ was calculated by applying the principles of Darcy's law using the hydraulic properties for time t. At any instant, the flow of water to and from a given layer was found from the gradient of hydraulic potential existing between that particular layer and its two adjacent layers. The source for irrigation water was simulated by keeping a given layer saturated at all times during irrigation. Figure 2 illustrates the salient features of the modeling concept. The abbreviations used in this figure are explained in Table 1.

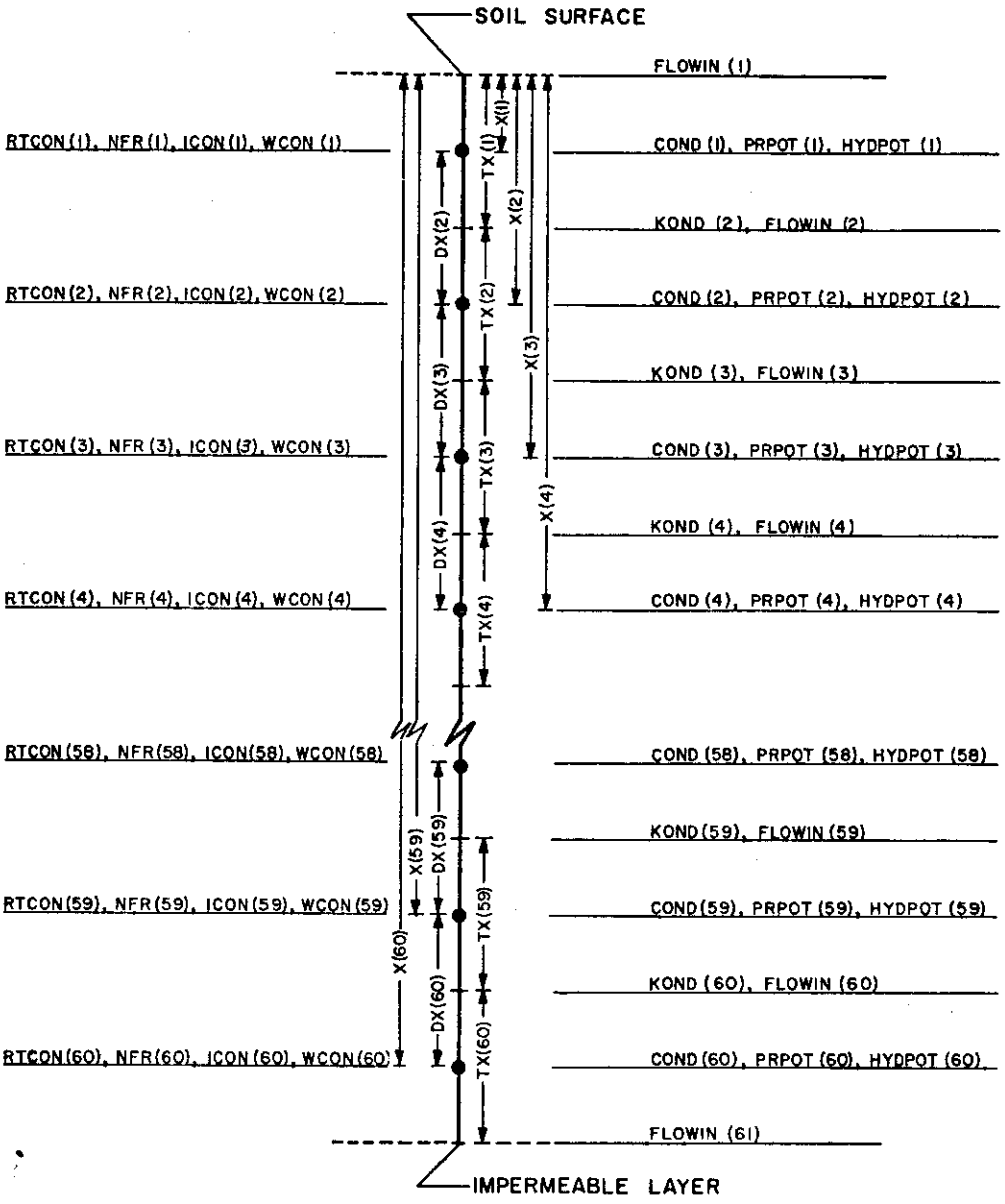

Figure 2 Physical modeling concept

Table 1 Definition of abbreviations used in Figure 2

FLOWIN(I) = Rate of flow across top boundary of Ith layer, cm/sec.

COND(I) = Hydraulic conductivity of Ith layer, cm/sec.

PRPOT(I) = Pressure potential of Ith layer, cm.

HYDPOT(I) = Hydraulic potential of Ith layer, cm.

KOND(I) = Average hydraulic conductivity across top boundary of Ith layer, cm/sec.

RTCON(I) = Root consumption rate of Ith layer, cm/sec.

NFR(I) = Net rate of flow into Ith layer, cm/sec.

ICON(I) = Initial water content of Ith layer, cm^3/cm^3.

WCON(I) = Water content of Ith layer, cm^3/cm^3.

X(I) = Gravitational potential of Ith layer measured from surface, cm.

TX(I) = Thickness of Ith layer, cm.

DX(I) = Distance between centers of (I-1)th and Ith layer, cm.

The root uptake rate (UPTAKE) was assumed to be a nonlinear function of the time of day, as shown in Figure 3, and proportional to the potential evapotranspiration for the same time, as illustrated in Figure 4 (Howell et al., 1971). A daily total uptake of 0.635 cm was used. The fraction of the UPTAKE attributed to a given layer was termed as the "root factor" (RFACT). The distribution of RFACT with root depth was taken to be a linearly decreasing function, as illustrated in Figure 5, in which the sum of the RFACT values for all

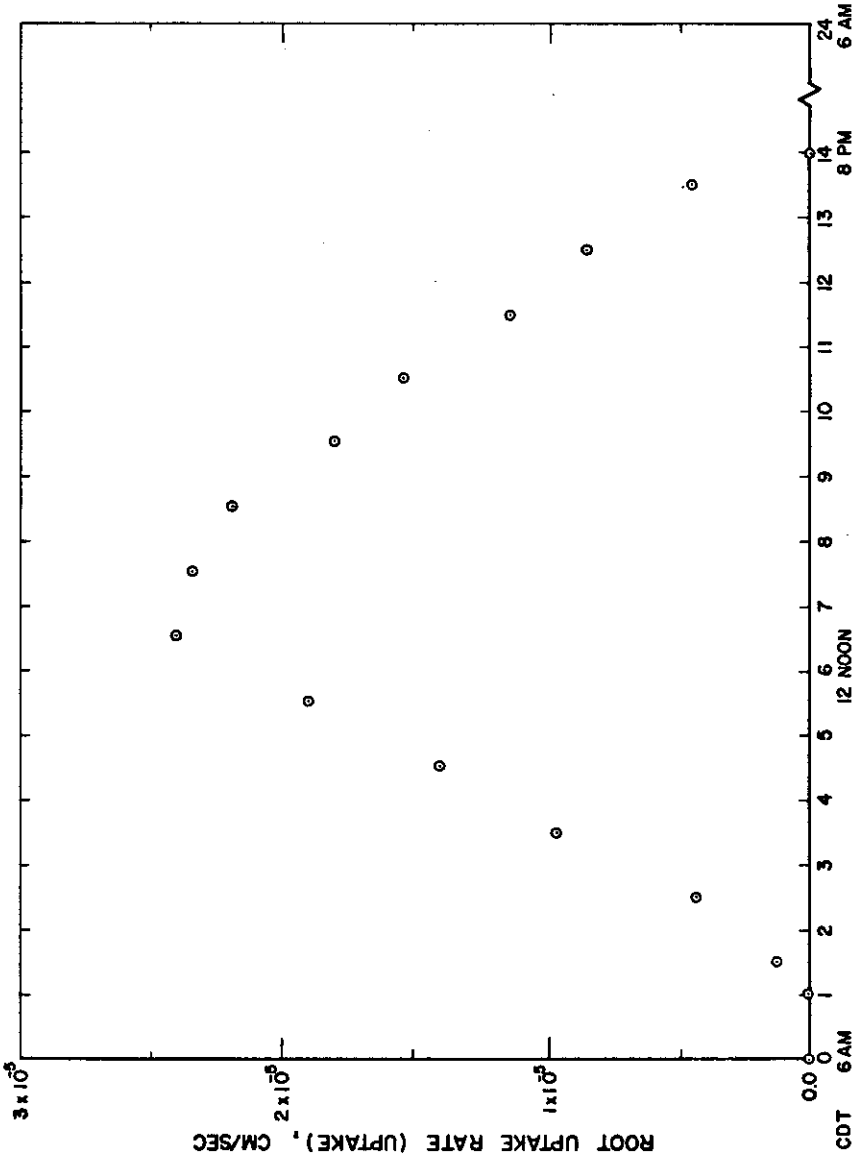

Figure 3 Distribution of root uptake rate with time of day

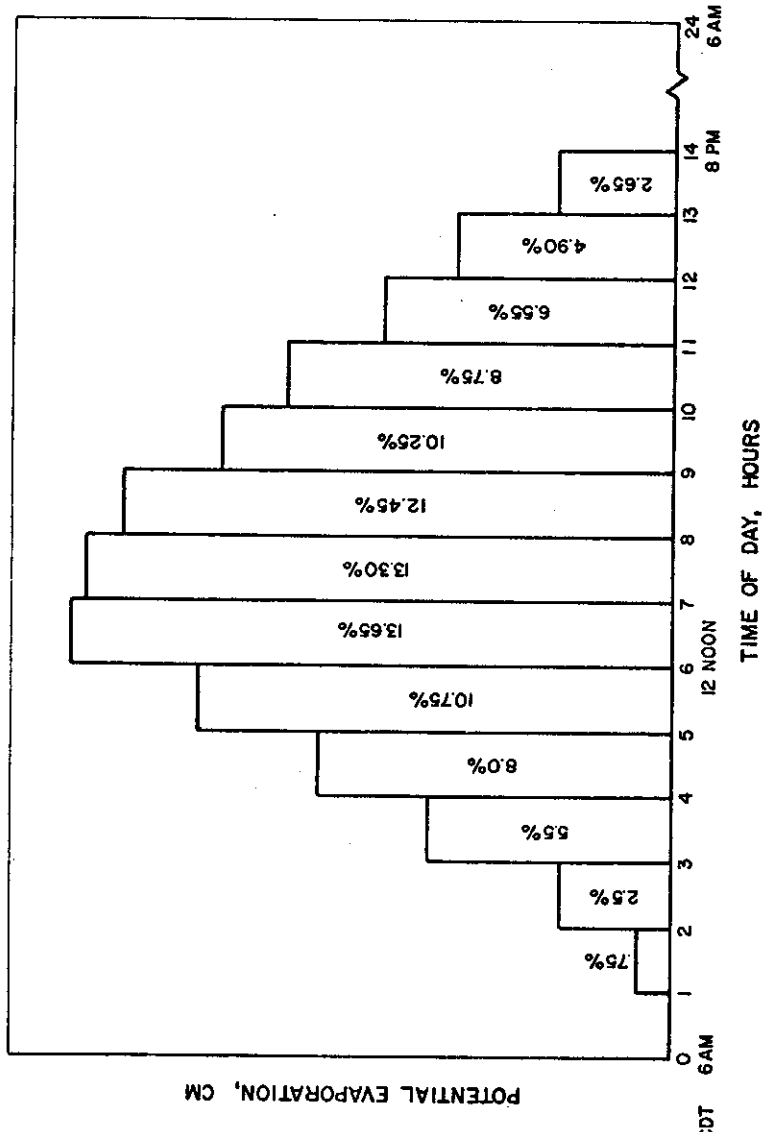

Figure 4 Potential evapotranspiration vs. time of day relationship

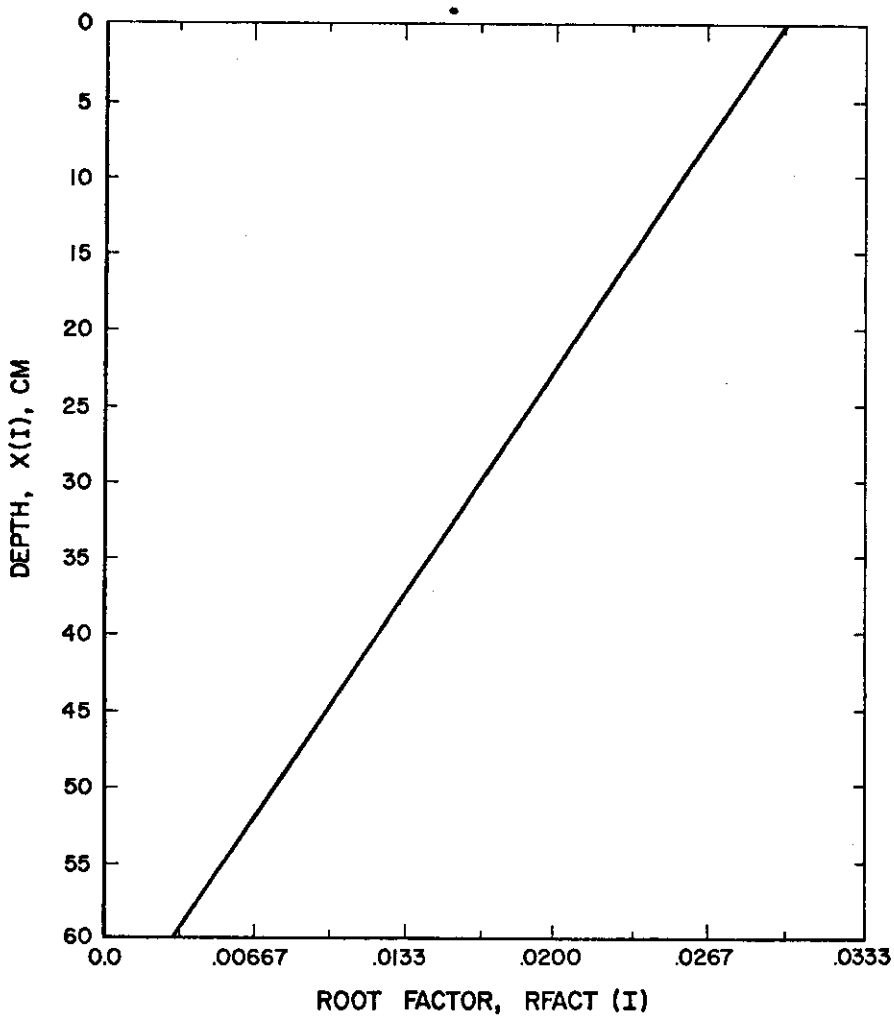

Figure 5 Distribution of the root factor (RFACT) with root depth (X)

the layers was equal to one. At any instant t, the root consumption rate (RTCON) at a given layer was equal to the UPTAKE for that time multiplied by the appropriate RFACT value. The time (RTIME) for calculating UPTAKE was set to zero after every 24 hours.

During each iteration, the net flow rate (NFR) to a given layer was calculated by applying the principle of conservation of mass. The incremental water content of each layer was then calculated by integrating its NFR, using the fourth order Runge-Kutta method of integration (METHOD RKS). This quantity was added to the previous initial water content to obtain the updated water content (WCON) as well as the corresponding hydraulic conductivity and pressure potential values for each layer. These values were then taken as the initial values for the next iteration, in a continuing updating procedure.

The infiltration rate (INRATE) from the source at a given time t was the sum of the absolute values of the flow rates across the top and bottom boundaries of the source layer. The total amount of water infiltrated (TOTINT) at time t was calculated by integrating the infiltration rate using METHOD RKS and adding to it the amount infiltrated prior to time t (PRETOT).

The computer program is shown in Table 2. Comment cards beginning with an asterisk were inserted to help explain the important aspects of the model. Some of the special features of S/360 CSMP are explained below.

The STORAGE statement allows one to specify that certain variable

Table 2 S/360 CSMP simulation of unsteady vertical infiltration of water from buried sources and redistribution in Yolo light clay

```
      STORAGE FLOWIN(200),PRPOT(200),COND(200),KOND(200),HYDPOT(200)
      STORAGE TX(200),DX(200),X(200),RTCON(200),RFACT(200)
/     DIMENSION NFR(200),WCON(200),ICON(200),W(200),WORK(200)
/     EQUIVALENCE (WCON1,WCON(1)),(NFR1,NFR(1)),(ICON1,ICON(1))
      FIXED I,NL,IPIPE,LOPART
      PARAMETER NL=60,IPIPE=21
*     NL=NUMBER OF LAYERS
*     IPIPE=LAYER NUMBER OF THE SOURCE
*     TX(I)=THICKNESS OF ITH LAYER, CM
*     DX(I)=DISTANCE BETWEEN CENTERS OF (I-1)TH AND ITH LAYER, CM
*     X(I)=GRAVIT. POTENTIAL OF ITH LAYER MEASURED FROM SURFACE, CM
*     PRPOT(I)=PRESSURE POTENTIAL OF ITH LAYER, CM
*     HYDPOT(I)=HYDRAULIC POTENTIAL OF ITH LAYER, CM
*     COND(I)=HYDRAULIC CONDUCTIVITY OF ITH LAYER, CM/SEC
*     KOND(I)=AV. HYDR. CONDUC. ACROSS TOP BOUNDARY OF ITH LAYER, CM/SEC
*     ICON(I)=INITIAL WATER CONTENT OF ITH LAYER, VOLUMETRIC FRACTION
*     WCON(I)=WATER CONTENT OF ITH LAYER, VOLUMETRIC FRACTION
*     FLOWIN(I)=RATE OF FLOW ACROSS TOP BOUNDARY OF ITH LAYER, CM/SEC
*     NFR(I)=NET RATE OF FLOW INTO ITH LAYER, CM/SEC
*     INRATE=RATE OF INFILTRATION INTO THE SOIL, CM/SEC
*     TOTINT=TOTAL AMOUNT OF INFILTRATION INTO THE SOIL, CM
*     RTCON(I)=ROOT CONSUMPTION RATE OF ITH LAYER, CM/SEC
*     RFACT(I)=ROOT FACTOR VALUE AT ITH LAYER
INITIAL
      NOSORT
      LOPART=IPIPE+1
      DO 10 I=1,NL
      TX(I)=1.0
10    CONTINUE
      X(1)=0.5*TX(1)
      DO 20 I=2,NL
      DX(I)=(TX(I-1)+TX(I))/2.0
      X(I)=X(I-1)+DX(I)
20    CONTINUE
      DO 30 I=1,NL
      PRPOT(I)=-140.0
      ICON(I)=NLFGEN(WCONT,PRPOT(I))
      COND(I)=NLFGEN(CONDT,ICON(I))
      RFACT(I)=AFGEN(RDISTN,X(I))
30    CONTINUE
*     RTIME=TIME OF DAY FOR CALCULATING ROOT CONSUMPTION, SEC
      RTIME=0.0
*     PRETOT=INITIAL VALUE OF TOTINT, CM
      PRETOT=0.0
      FLOWIN(1)=0.0
      FLOWIN(NL+1)=0.0
*     SWITCH=1 MEANS THAT INFILTRATION CYCLE IS 'ON'
*     SWITCH=2 MEANS THAT DRYING CYCLE IS 'ON'
      SWITCH=1
      KOND(1)=COND(1)
      HYDPOT(1)=PRPOT(1)-X(1)
      DO 40 I=1,NL
      WRITE(6,41)X(I)
41    FORMAT(1H ,F7.2)
```

Table 2 (continued)

```
40      CONTINUE
        FUNCTION RDISTN=0.0,0.03,15.0,0.02333,30.0,0.01666,45.0,0.01,...
        60.0,0.00333
        FUNCTION CONSUM=0.0,0.0,3600.0,0.0,5400.0,0.000001321,...
        9000.0,0.00000441,12600.0,0.0000097,16200.0,0.00001411,...
        19800.0,0.00001895,23400.0,0.00002405,27000.0,0.00002345,...
        30600.0,0.00002194,34200.0,0.00001805,37800.0,0.00001545,...
        41400.0,0.00001155,45000.0,0.00000864,48600.0,0.00000467,...
        50400.0,0.0,86400.0,0.0
*
*       SOIL - YOLO LIGHT CLAY
*
        FUNCTION WCONT=-5000000.0,0.025,-280000.0,0.05,-61000.0,0.075,...
        -17700.0,0.10,-8250.0,0.125,-4000.0,0.15,-1330.0,0.20,...
        -660.0,0.2375,-620.0,0.2408,-580.0,0.2442,...
        -540.0,0.2481,-500.0,0.2520,-460.0,0.2562,-420.0,0.2612,...
        -380.0,0.2662,-340.0,0.2725,-300.0,0.2787,-260.0,0.2862,...
        -220.0,0.2950,-180.0,0.3050,-140.0,0.3200,-100.0,0.3400,...
        -80.0,0.3500,-60.0,0.3800,-40.0,0.4200,-20.0,0.4600,...
        -12.0,0.4760,-8.0,0.4840,-4.0,0.4920,0.0,0.5000
        FUNCTION CONDT=.0,.0,.2375,.0000000520,.2408,.0000000552,...
        .2442,.0000000600,.2481,.0000000650,.2520,.0000000685,...
        .2562,.0000000750,.2612,.0000000824,.2662,.0000000910,...
        .2725,.0000001025,.2787,.0000001180,.2862,.0000001350,...
        .2950,.0000001600,.3050,.0000001900,.3200,.0000002600,...
        .3400,.0000004100,.3500,.0000005300,.3800,.0000009500,...
        .4200,.0000019100,.4600,.0000040000,.4760,.0000055500,...
        .4840,.0000064000,.4920,.0000077000,.5000,.0000092500
        FUNCTION POT=.025,-5000000.0,.050,-280000.0,.075,-61000.0,...
        .100,-17700.0,.125,-8250.0,.150,-4000.0,.200,-1330.0,...
        .2375,-660.0,.2408,-620.0,.2442,-580.0,...
        .2612,-420.0,.2662,-380.0,.2725,-340.0,.2787,-300.0,...
        .2862,-260.0,.2950,-220.0,.3050,-180.0,.3200,-140.0,...
        .3400,-100.0,.3500,-80.0,.3800,-60.0,.4200,-40.0,...
        .4600,-20.0,.4760,-12.0,.4840,-8.0,.4920,-4.0,.5000,0.0
        WCON1=INTGRL(ICON1,NFR1,60)
DYNAMIC
        NOSORT
*       KEEP=0 IS AN INVALID ITERATION AND HENCE KEPT OUT OF RTIME
        IF(KEEP.EQ.0) GO TO 50
        RTIME=RTIME+DELT
50      CONTINUE
*       SETTING RTIME BACK TO ZERO AFTER EVERY 24 HOURS
        IF(RTIME.GE.86400.0) GO TO 60
        GO TO 70
60      RTIME=(RTIME-86400.0)
*       UPTAKE=ROOT UPTAKE RATE AT A GIVEN TIME
70      UPTAKE=NLFGEN(CONSUM,RTIME)
        DO 80 I=1,NL
        RTCON(I)=(UPTAKE)*(RFACT(I))
80      CONTINUE
        IF(SWITCH.EQ.2) GO TO 140
        WCON(IPIPE)=0.50
        COND(IPIPE)=0.00000925
        KOND(IPIPE)=0.00000925
        KOND(IPIPE+1)=0.00000925
        PRPOT(IPIPE)=0.0
        DO 90 I=2,NL
```

Table 2 (continued)

```
      IF(I.EQ.IPIPE) GO TO 90
      IF(I.EQ.LOPART) GO TO 90
      KOND(I)=(COND(I)+COND(I-1))/2.0
90    CONTINUE
      DO 100 I=2,NL
      HYDPOT(I)=PRPOT(I)-X(I)
      FLOWIN(I)= (HYDPOT(I-1)-HYDPOT(I))*KOND(I)/DX(I)
100   CONTINUE
      INRATE=ABS(FLOWIN(IPIPE))+ABS(FLOWIN(IPIPE+1))
      TOTINT=INTGRL(PRETOT,INRATE)
*     CALCULATING NET WATER CONTENT
      DO 110 I=1,NL
      IF(I.EQ.IPIPE) GO TO 110
      NFR(I)=FLOWIN(I)-FLOWIN(I+1)-RTCON(I)
110   CONTINUE
      DO 120 I=1,NL
      W(I)=WCON(I)
      WCON(I)=LIMIT(0.08,0.50,W(I))
      WORK(I)=NFR(I)
120   CONTINUE
      DO 130 I=1,NL
      IF(I.EQ.IPIPE) GO TO 130
      COND(I)=NLFGEN(CONDT,WCON(I))
      PRPOT(I)=NLFGEN(POT,WCON(I))
130   CONTINUE
      GO TO 200
140   DO 150 I=2,NL
      KOND(I)=(COND(I)+COND(I-1))/2.0
      HYDPOT(I)=PRPOT(I)-X(I)
      FLOWIN(I)=(HYDPOT(I-1)-HYDPOT(I))*KOND(I)/DX(I)
150   CONTINUE
      INRATE=0.0
      DO 160 I=1,NL
      NFR(I)=FLOWIN(I)-FLOWIN(I+1)-RTCON(I)
160   CONTINUE
      DO 170 I=1,NL
      W(I)=WCON(I)
      WCON(I)=LIMIT(0.08,0.50,W(I))
      WORK(I)=NFR(I)
170   CONTINUE
      DO 180 I=1,NL
      COND(I)=NLFGEN(CONDT,WCON(I))
      PRPOT(I)=NLFGEN(POT,WCON(I))
180   CONTINUE
200   WCON1=WCON(1)
      WCON2=WCON(2)
      WCON3=WCON(3)
      WCON4=WCON(4)
      WCON5=WCON(5)
      WCON6=WCON(6)
      WCON7=WCON(7)
      WCON8=WCON(8)
      WCON9=WCON(9)
      WCON10=WCON(10)
      WCON11=WCON(11)
      WCON12=WCON(12)
      WCON13=WCON(13)
      WCON14=WCON(14)
```

Table 2 (continued)

```
WCON15=WCON(15)
WCON16=WCON(16)
WCON17=WCON(17)
WCON18=WCON(18)
WCON19=WCON(19)
WCON20=WCON(20)
METHOD RKS
PRINT WCON2,WCON3,WCON4,WCON5,WCON6,WCON7,WCON8,WCON9,WCON10,...
WCON11,WCON12,WCON13,WCON14,WCON15,WCON16,WCON17,WCON18,...
WCON19,WCON20,RTIME,DELT,TOTINT,INRATE
RELERR WCON1=0.10
RELERR TOTINT=0.10
TIMER DELT=25.0, PRDEL=3600.0, FINTIM=1000000.0
FINISH WCON9=0.35
CONTINUE
RESET FINISH
PARAMETER SWITCH=2
RELERR WCON1=0.10
RELERR TOTINT=0.10
TIMER PRDEL=3600.0, FINTIM=5000000.0
FINISH WCON20=0.35
END
STOP
```

names, which appear on that card, are subscripted and the number within the parentheses must be the maximum number of storage locations necessary to contain data for the corresponding variable. The FIXED statement allows declaration of the listed variables as being integer numbers. The PARAMETER card allows variables to have assigned values.

The program has two primary sections --- INITIAL and DYNAMIC. The INITIAL segment is performed just once before the simulation runs, whereas the DYNAMIC segment computations are performed during each iteration. The NOSORT statement after the INITIAL and DYNAMIC labels declares that all the subsequent structure statements within the section are to be considered procedural, thus permitting unrestricted use of FORTRAN conditional logic and branching.

The hydraulic properties of the soil were defined in the INITIAL section by nonlinear function generators (NLFGEN) which provided Lagrange quadratic interpolation between consecutive points. The X and Y coordinates of the function points were entered sequentially following the function label and the symbolic name of the function (e.g., FUNCTION WCONT). The symbolic names WCONT, CONDT, and POT represented the pressure potential vs. water content, water content vs. hydraulic conductivity, and water content vs. pressure potential relationships, respectively, for the soil. The functions RDISTN and CONSUM, respectively, specify the depth vs. root factor and the time of day vs. root consumption rate relationships. The statement

```
WCON1 = INTGRL (ICON1, NFR1, 60)
```

specifies to the S/360 CSMP translator that the total number of

integrators indicated in the DYNAMIC section of the model should be augmented by the quantity 60. The symbols WCON1, ICON1, and NFR1, which are the output, the initial value, and the integrand, respectively, are dummy variables EQUIVALENCEd to the first elements of the corresponding vector arrays, WCON, ICON, and NFR.

The DYNAMIC section of the program may be divided, in order to explain its contents, into four segments. The first segment beginning right after the NOSORT statement ends in the statement numbered 80. In this part, the root consumption rate at time t is computed for each layer. The system variable KEEP equal to zero means a trial evaluation; hence, it is kept out of the calculation for root consumption time (RTIME). The second segment, which ends in statement numbered 130, constitutes the irrigation cycle. This segment is run through only when SWITCH = 1, i.e., irrigation is on. The drying cycle, or the third segment, consists of the part of the program from statement numbers 140 through 180. When SWITCH = 2, i.e., during the drying period, the simulation skips the second segment for calculation. The fourth and last segment which consists of the rest of the program is common to both the irrigation and drying cycle.

The METHOD RKS provided the variable step fourth-order Runge-Kutta method of integration. In this method, the integration intervals are adjusted to meet selected error criteria. The error in integration is set by the relative error (RELERR) and the absolute error (ABSERR) of the integral. When any of these errors is specified for any integrator, the last error specified before an END or CONTINUE

card is applied to all integrators that are unspecified. The PRINT statement enabled printing of the selected output variables at time intervals indicated by the OUTDEL value in the TIMER card. FINTIM specified the maximum simulation value for time, the independent variable.

The FINISH card allowed definition of terminating conditions other than FINTIM. Use of CONTINUE cards enabled automatic sequencing of irrigation and drying cycles. It permitted the simulation to accept changed data and control statements, without resetting time, and to continue the run. A combination of END and STOP cards specified termination of the sequence.

The fourth order variable-step Runge-Kutta method of integration (METHOD RKS) is one of the seven different routines that are available in S/360 CSMP to perform the integration operation. The variable-step method was preferred over a fixed-step method because it provides the capacity to adjust the integration intervals to satisfy specified error bounds. The error in integration is set by the value given to the relative error (RELERR) and absolute error (ABSERR) of the output. When nothing is mentioned in the program about the error, the relative and absolute errors are set by the system at 0.0001 and 0.001, respectively. This device allows specification of the desired error in integration and also elimination of the possibility of unstable solutions.

In the variable-step Runge-Kutta method, the integration interval is reduced to satisfy the following criterion:

$$\frac{|Y_{t+\Delta t} - Y_s|}{A + R.|Y_{t+\Delta t}|} \cong \frac{\text{Error}}{A + R.|Y_{t+\Delta t}|} \leq 1, \qquad (9)$$

where Y_s is $Y_{t+\Delta t}$ calculated by Simpson's rule, and A and R are the absolute and relative errors corresponding to the particular integrator value. Further information on the language are available in the CSMP manual (IBM, 1967).

Infiltration through the Surface

The development of a dynamic computer program capable of simulating vertical infiltration through the surface was the logical step to precede the evolvement of the dynamic model for infiltration from buried sources. Here, the plant-root consumption of water was not considered. The availability of a theoretical solution due to Philip (1957a, 1957b) provided an opportunity for comparison.

The computer program is shown in Table 3. The basic modeling concept and the boundary conditions in this case were exactly the same as described earlier. This program differed from the program for infiltration from buried sources, as illustrated in Table 2 (p. 19-22), in that here the source was not below but at the surface, and that it did not consider consumption of water by plant roots during the infiltration process. A pressure potential of -660.0 cm of water, which was uniform with depth, was used as the initial condition. A soil mass 50-cm deep and divided into layers each one-centimeter thick was used. Simulation data were obtained for three different soils -- Yolo light clay, Adelanto loam, and Pachappa loam.

Table 3 S/360 CSMP simulation of unsteady vertical infiltration through surface into unsaturated Yolo light clay

```
      STORAGE PRPOT(200),COND(200),KOND(200),HYDPOT(200),FLOWIN(200)
      STORAGE TX(200),DX(200),X(200)
/     DIMENSION NFR(200),WCON(200),ICON(200),W(200),WORK(200)
/     EQUIVALENCE (WCON1,WCON(1)),(NFR1,NFR(1)),(ICON1,ICON(1))
      FIXED I,NL,IPIPE,LOPART
      PARAMETER NL=50,IPIPE=1
*     NL=NUMBER OF LAYERS
*     IPIPE=LAYER NUMBER OF THE SOURCE
*     TX(I)=THICKNESS OF ITH LAYER, CM
*     DX(I)=DISTANCE BETWEEN CENTERS OF (I-1)TH AND ITH LAYER, CM
*     X(I)=GRAVIT. POTENTIAL OF ITH LAYER MEASURED FROM SURFACE, CM
*     PRPOT(I)=PRESSURE POTENTIAL OF ITH LAYER, CM
*     HYDPOT(I)=HYDRAULIC POTENTIAL OF ITH LAYER, CM
*     COND(I)=HYDRAULIC CONDUCTIVITY OF ITH LAYER, CM/SEC
*     KOND(I)=AV. HYDR. CONDUC. ACROSS TOP BOUNDARY OF ITH LAYER, CM/SEC
*     ICON(I)=INITIAL WATER CONTENT OF ITH LAYER, VOLUMETRIC FRACTION
*     WCON(I)=WATER CONTENT OF ITH LAYER, VOLUMETRIC FRACTION
*     FLOWIN(I)=RATE OF FLOW ACROSS TOP BOUNDARY OF ITH LAYER, CM/SEC
*     NFR(I)=NET RATE OF FLOW INTO ITH LAYER, CM/SEC
*     INRATE=RATE OF INFILTRATION INTO THE SOIL, CM/SEC
*     TOTINT=TOTAL AMOUNT OF INFILTRATION INTO THE SOIL, CM
INITIAL
      NOSORT
      DO 10 I=1,NL
      TX(I)=1.0
10    CONTINUE
      X(1)=0.5*TX(1)
      DO 20 I=2,NL
      DX(I)=(TX(I-1)+TX(I))/2.0
      X(I)=X(I-1)+DX(I)
20    CONTINUE
      DO 30 I=1,NL
      PRPOT(I)=-660.0
      ICON(I)=NLFGEN(WCONT,PRPOT(I))
      COND(I)=NLFGEN(CONDT,ICON(I))
30    CONTINUE
      PRETOT=0.0
      LOPART=IPIPE+1
*     BOUNDARY CONDITIONS
      FLOWIN(1)=0.0
      FLOWIN(NL+1)=0.0
      WCON(IPIPE)=0.500
      PRPOT(IPIPE)=0.0
      KOND(IPIPE)=0.00000925
      KOND(IPIPE+1)=0.00000925
      HYDPOT(1)=PRPOT(1)-X(1)
*     SOIL - YOLO LIGHT CLAY
      FUNCTION WCONT=-1330.,.20,-660.,.2375,-620.,.2408,-580.,.2442,...
      -540.,.2481,-500.,.2520,-460.,.2562,-420.,.2612,-380.,.2662,...
      -340.,.2725,-300.,.2787,-260.,.2862,-220.,.2950,-180.,.3050,...
      -140.,.3200,-100.,.3400,-80.,.3500,-60.,.3800,-40.,.4200,...
      -20.,.4600,-12.,.4760,-8.,.4840,-4.,.4920,0.0,.5000
      FUNCTION CONDT=.0,.0,.2375,.0000000520,.2408,.0000000552,...
```

Table 3 (continued)

```
      .2442,.0000000600,.2481,.0000000650,.2520,.0000000685,...
      .2562,.0000000750,.2612,.0000000824,.2662,.0000000910,...
      .2725,.0000001025,.2787,.0000001180,.2862,.0000001350,...
      .2950,.0000001600,.3050,.0000001900,.3200,.0000002600,...
      .3400,.0000004100,.3500,.0000005300,.3800,.0000009500,...
      .4200,.0000019100,.4600,.0000040000,.4760,.0000055500,...
      .4840,.0000064000,.4920,.0000077000,.5000,.0000092500
      FUNCTION POT=.200,-1330.,.2375,-660.,.2408,-620.,.2442,-580.,...
      .2481,-540.,.2520,-500.,.2562,-460.,.2612,-420.,.2662,-380.,...
      .2725,-340.,.2787,-300.,.2862,-260.,.2950,-220.,.3050,-180.,...
      .3200,-140.,.3400,-100.,.3500,-80.,.3800,-60.,.4200,-40.,...
      .4600,-20.,.4760,-12.,.4840,-8.,.4920,-4.,.5000,0.0
      WCON1=INTGRL(ICON1,NFR1,50)
DYNAMIC
      NOSORT
      DO 40 I=2,NL
      IF(I.EQ.IPIPE) GO TO 40
      IF(I.EQ.LOPART) GO TO 40
      KOND(I)=(COND(I)+COND(I-1))/2.0
40    CONTINUE
      DO 50 I=2,NL
      HYDPOT(I)=PRPOT(I)-X(I)
      FLOWIN(I)= (HYDPOT(I-1)-HYDPOT(I))*KOND(I)/DX(I)
50    CONTINUE
      INRATE=ABS(FLOWIN(IPIPE))+ABS(FLOWIN(IPIPE+1))
      TOTINT=INTGRL(PRETOT,INRATE)
      DO 60 I=1,NL
      IF(I.EQ.IPIPE) GO TO 60
      NFR(I)=FLOWIN(I)-FLOWIN(I+1)
60    CONTINUE
*     LIMITING THE LOWEST AND HIGHEST POSSIBLE WATER CONTENTS
      DO 70 I=1,NL
      W(I)=WCON(I)
      WCON(I)=LIMIT(0.0,0.500,W(I))
      WORK(I)=NFR(I)
70    CONTINUE
*     UPDATING HYDRAULIC CONDUCTIVITY AND PRESSURE POTENTIAL
      DO 80 I=1,NL
      IF(I.EQ.IPIPE) GO TO 80
      COND(I)=NLFGEN(CONDT,WCON(I))
      PRPOT(I)=NLFGEN(POT,WCON(I))
80    CONTINUE
      WCON2=WCON(2)
      METHOD RKS
      PRTPLT WCON2,TOTINT(INRATE)
      TIMER DELT=2.0, OUTDEL=1000.0, FINTIM=100000.0
      END
      STOP
```

For Yolo light clay, the hydraulic characteristics, as shown in Figures 6 and 7, were taken from the work of Moore (1939) as used by Philip (1969). For the other two soils, the data given by Jackson et al. (1965), Figures 8 and 9, were used. In each case, infiltration was continued long enough to ensure penetration of the wetting front to a depth of 40 cm or more below the surface.

Infiltration from Buried Sources and Redistribution

The computer model, as presented in Table 2 (p. 19-22), was used for the dynamic simulation of vertical infiltration and redistribution during the drying cycle in a homogeneous unsaturated soil. The source was located below the soil surface and consumption of water by plant roots was taken into account. Yolo light clay soil 60-cm deep was used. The soil was divided into layers each of which was one centimeter thick. A root depth of 60 cm was used. A daily total root consumption of 0.635 cm of water, distributed nonlinearly with the time of day, as illustrated in Figure 3 (p. 15), was used.

Three levels of the source, 10, 20, and 30 cm below the soil surface, were used. Two sets of simulation data were obtained. The initial water content was maintained uniform at 0.2375 (cm^3/cm^3) for the first set and at 0.32 (cm^3/cm^3) for the other. In each case, one irrigation cycle was first performed which was followed by one drying cycle. The duration of each cycle was monitored by the specified water content value at a selected point, called the control point.

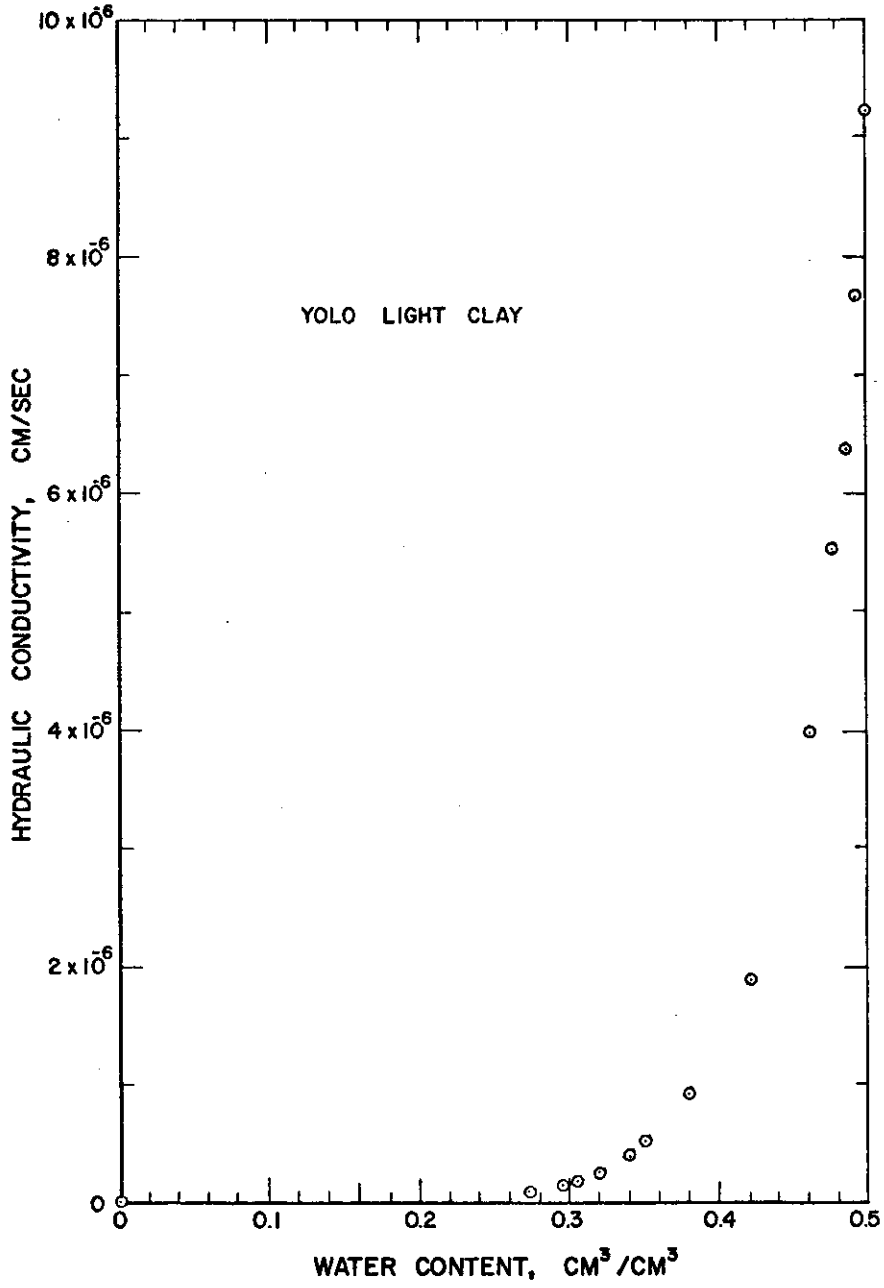

Figure 6 Water content vs. hydraulic conductivity relationship for Yolo light clay

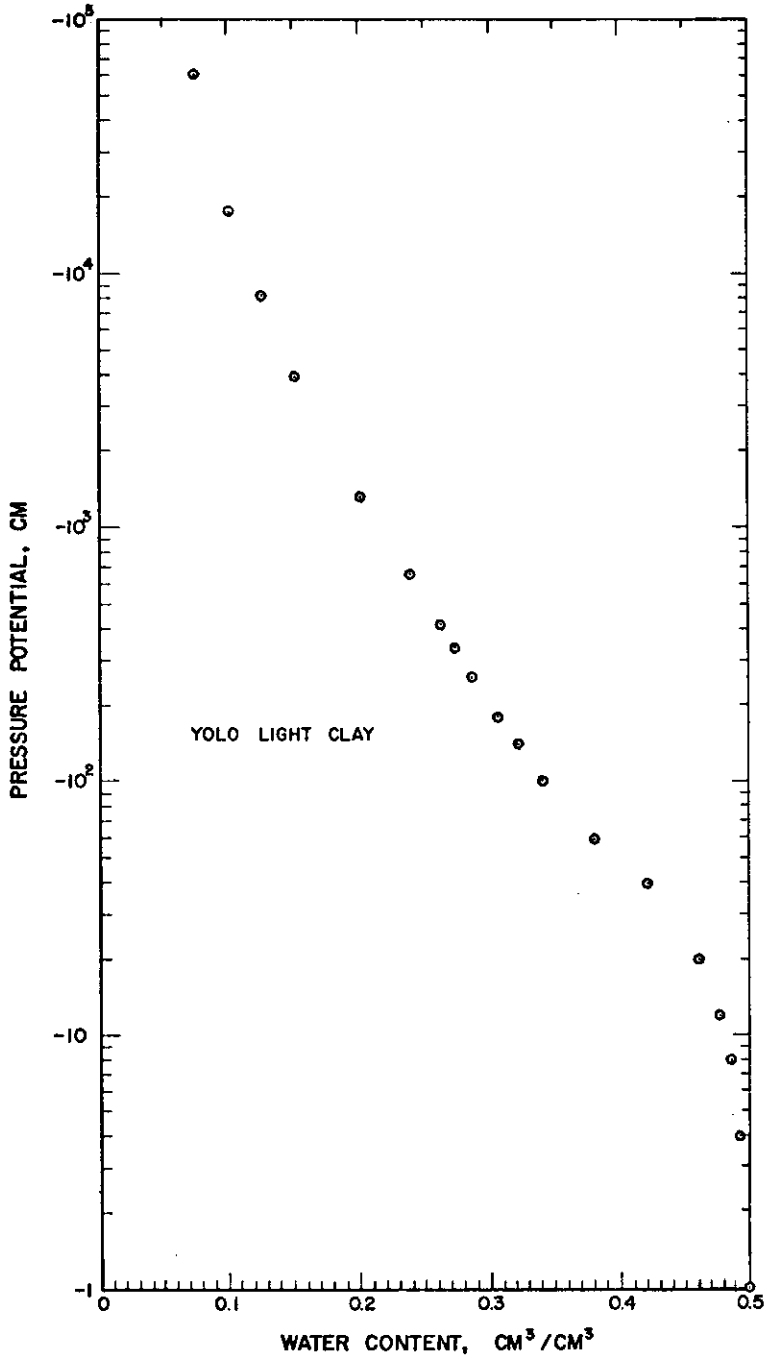

Figure 7 Water content vs. pressure potential relationship for Yolo light clay

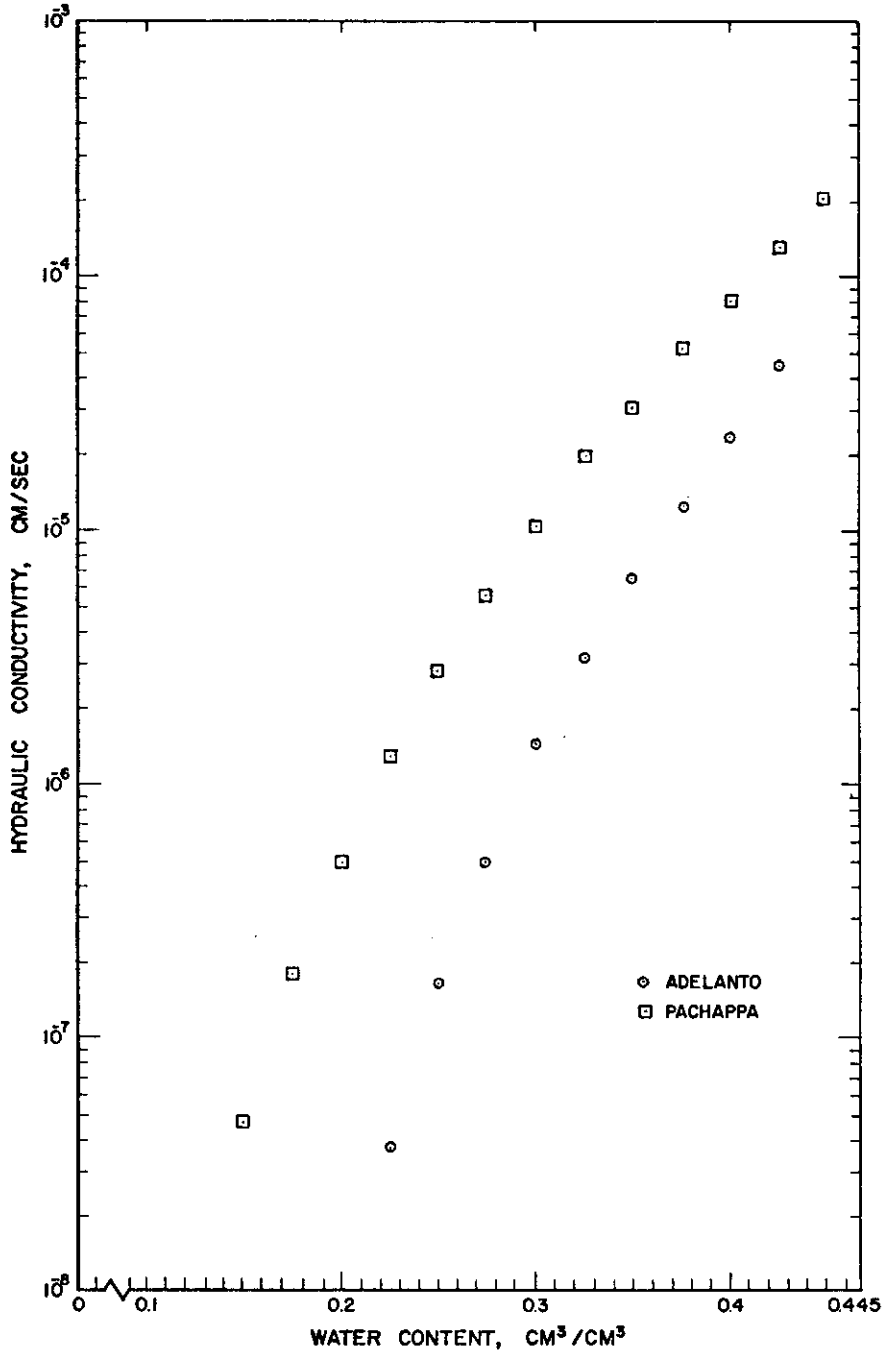

Figure 8 Water content vs. hydraulic conductivity relationship for Adelanto and Pachappa loam

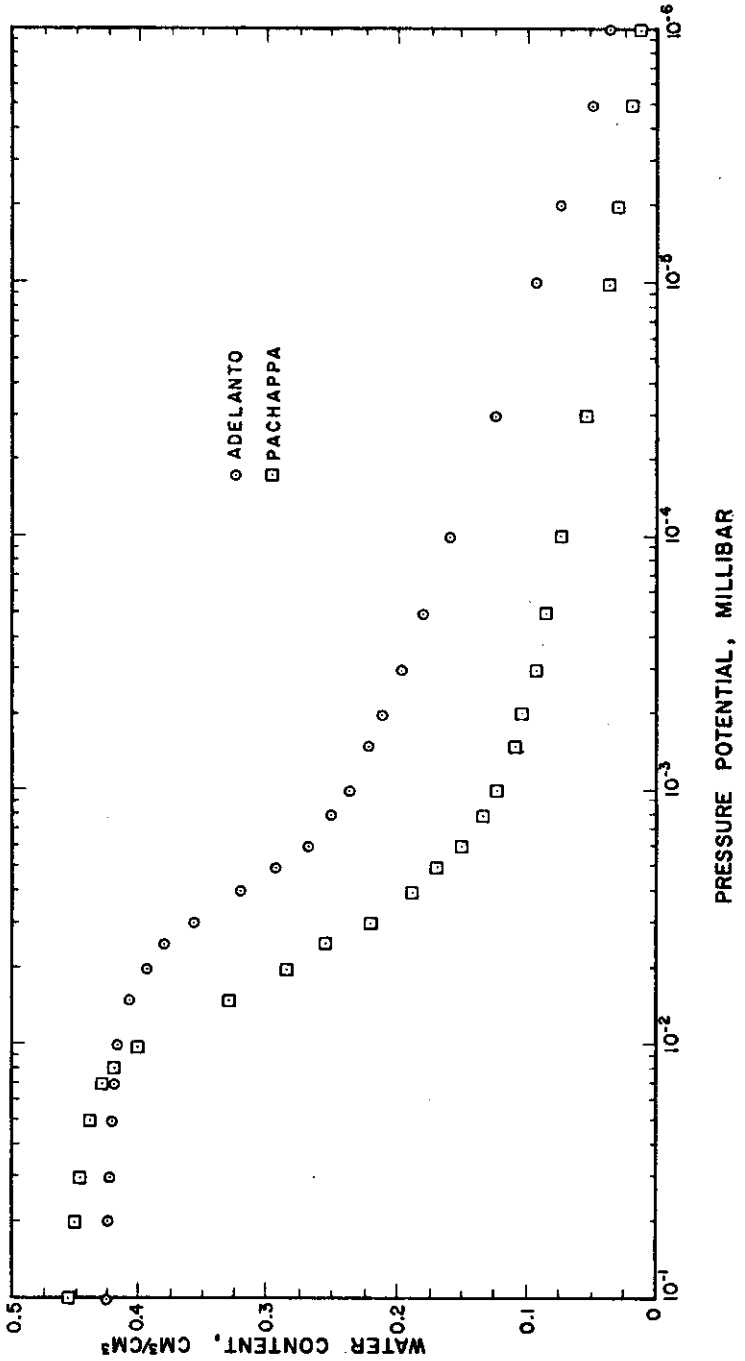

Figure 9 Pressure potential vs. water content relationship for Adelanto and Pachappa loam

In the first set of simulation, both the cycles in each run were monitored by the same control point. Two, three, and four simulation runs were performed for source locations at 10, 20, and 30 cm, respectively. For each source, the first control point was located at four centimeters above the center of the source whereas the others were located two centimeters apart toward the soil surface. The cut-off water content values at the control points for the irrigation and the drying cycle were specified at 0.35 (cm^3/cm^3) and 0.32 (cm^3/cm^3), respectively.

In the second set, one simulation run was performed for the 10-cm source level with the control point for the irrigation cycle specified at eight centimeters above the center of the source. Two simulation runs, the irrigation cycle control point located at eight centimeters above the center of the source for one and at 12 cm above for the other, were performed for each of the other two source levels. In each case, the control point for the drying cycle was specified at one centimeter above the center of the source. The cut-off water content value at the control points for both the cycles were set at 0.35 (cm^3/cm^3) for each simulation in this set.

CHAPTER IV

SUBIRRIGATION DESIGN CRITERIA

General Considerations

The design considerations for a subirrigation system, assuming a constant source, revolve around three basic questions: (a) At what depth should the source be located? (b) When should one irrigate? (c) How much water should one apply? Question (a) calls for determining the optimum depth of the source for a particular soil and crop and (b) and (c) raise the question of irrigation scheduling.

The optimum depth of the source is the one that assures the following criteria:

(i) Adequate supply of water, as needed in different depths of the root zone, must be supplied.

(ii) The overall irrigation efficiency should be as high as possible.

Irrigation efficiency, in a conventional system, can be divided into six segments: (1) water-conveyance efficiency, (2) water-application efficiency, (3) water-storage efficiency, (4) consumptive-use efficiency, (5) water-use efficiency, and (6) water-distribution efficiency (Israelsen and Hansen, 1965). Whereas it is usually difficult to maintain a high degree of efficiency in all the segments in a conventional surface irrigation system and, as such, a careful balance between them is necessary, subirrigation ensures a very high

degree of efficiency in the first four segments (assuming negligible surface evaporation and deep percolation). The water-use efficiency and the water-distribution efficiency are the areas where particular attention should be given in designing an efficient subirrigation system.

The concept of water-distribution efficiency, as it applies to a conventional system, is a measure of the evenness of distribution in a horizontal axis along the length of run. The distribution along the vertical direction is more important in a subirrigation system. For the one-dimensional system considered in this study, the vertical distribution pattern is the only consideration.

The effect of gravity is dependent upon the degree of saturation in a given soil. Since the initial water content is assumed to be uniform with depth, gravity causes more water to infiltrate in the downward direction than in the upward direction. This, along with the fact that the root consumption rate decreases with depth, suggests that a higher efficiency can be expected only when the source is located above the middle of the root zone.

From the operational point of view, however, for a subirrigation system to be installed in the field, the source should be located below the tillage depth. From that consideration, 30 cm should perhaps be regarded as the minimum depth of the source in a field where normal tillage operations are done. For controlled plots (e.g., green house), however, a shallower depth may be workable.

Two New Concepts

In order to evaluate the effectiveness of vertical water distribution in a subirrigation system, two new concepts are introduced. They are: (1) Availability Coefficient, and (2) Proportionality Coefficient. Before defining these concepts, it is necessary to explain the term "desirable water content profile." It is assumed that for a given crop and soil, there exists a water content profile with depth which is optimum for crop production. This profile is termed as the "desirable water content profile." In a subirrigation system, it is desirable to maintain water content profiles as close to this ideal profile as possible. The definition of the coefficients are given below.

$$\underline{\text{Availability Coefficient}},\ C_a = 1.0 - \frac{1}{N}\left(\left|\sum\frac{\Delta xP_i}{DW_i} - \sum\frac{\Delta xn_i}{DW_i}\right|\right),$$

where ΔxP_i = positive value of the deviation of water content of ith observation from the desired water content at that point,

Δxn_i = negative value of the deviation of water content of ith observation from the desired water content at that point,

DW_i = desired water content of ith observation,

and N = number of observations.

The availability coefficient, C_a, is a measure of the degree of excess or deficiency of water in the root zone with respect to the amount represented by the desirable water content profile. The

maximum value of the coefficient is 1.0.

$$\underline{\text{Proportionality Coefficient}},\ C_p = 1.0 - \frac{1}{N}\left(\sum \frac{\Delta x_i}{DW_i}\right),$$

where Δx_i = absolute deviation of water content of ith observation from the desired water content at that point,

and other parameters are the same as defined earlier.

The proportionality coefficient, C_p, is indicative of the average proximity of a given water content profile to the desirable profile. When the deviation from the ideal profile is zero, the proportionality coefficient is 1.0.

It is the combined effect of the two coefficients, rather than any one of them, that is important in evaluating the effectiveness of vertical water distribution in a subirrigation system. This is because, for an optimum design situation, both adequacy of supply as well as efficiency of the system are equally important. Figure 10 contains seven illustrative profiles indicating the relative merits of each. Examples (a) and (b) are cases of excess water near the bottom and the values of the coefficients are very low. Examples (c) and (d) have the same values of C_a and of C_p; but judging from the root extraction pattern shown in Figure 5 (p.17) and the effect of gravity, example (d) would be the case of better distribution. Out of examples (e) and (f), both of which have the same values of C_a and C_p, one may be tempted to choose example (e) over (f) because of its sufficiency of water applied. But a correct decision can only be made

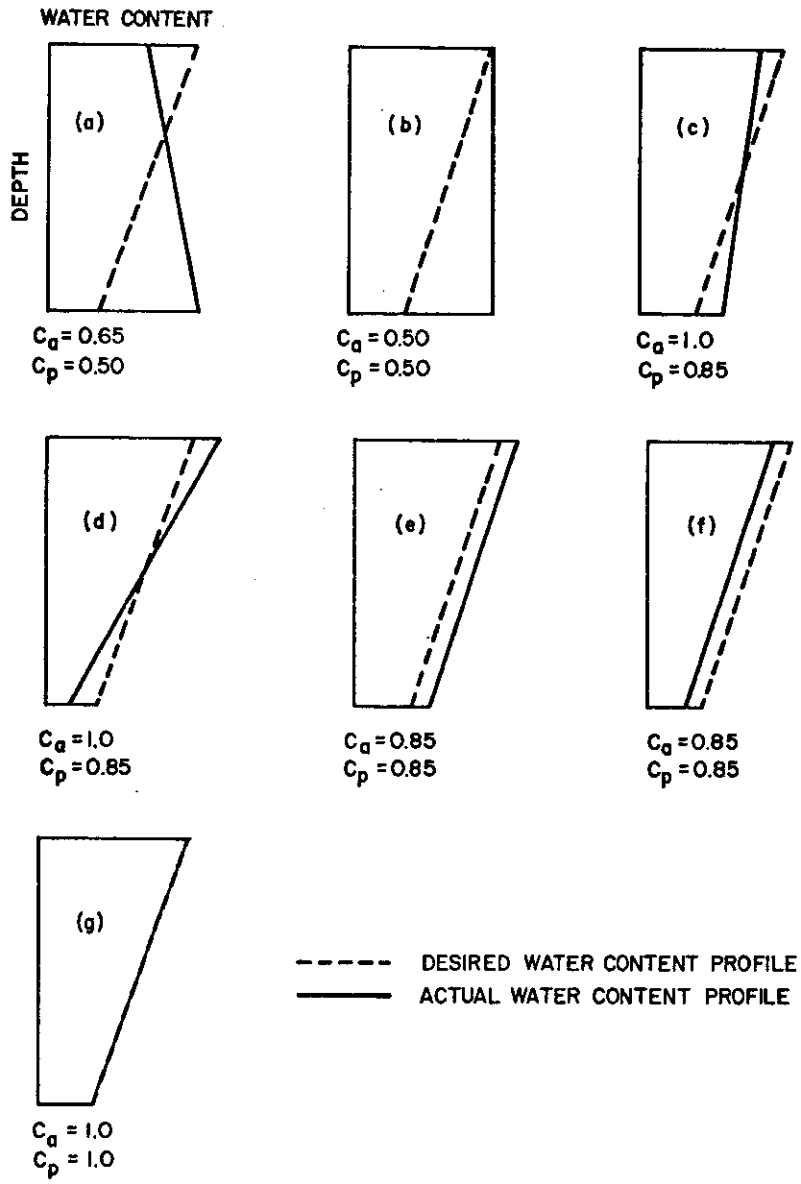

Figure 10 Illustration of the availability coefficient, C_a, and the proportionality coefficient, C_p

when the comparative effects of both the cases on crop yield are known. It is interesting to note that although in each of examples (c), (d), and (g) the value of C_a = 1.0, it is only in (g) that C_p has a value of 1.0.

The ideal profile that is desirable for optimum yield is likely to be dependent on the crop as well as the soil. It is expected that this profile would be a function of the root extraction pattern for a given soil and crop. Field experiments are necessary for determining the nature of the ideal profile.

A numerical example, which illustrates the technique of computation of the coefficients, C_a and C_p, is furnished below.

Example. The water content values of the desirable profile and the actual profile measured at indicated depths are given in Table 4. The values of C_a and C_p are computed also.

Table 4 Example of computation of the availability coefficient, C_a, and the proportionality coefficient, C_p

Depth (cm)	Measured water content (cm^3/cm^3)	Water content of desired profile (cm^3/cm^3)	(2-3) (cm^3/cm^3)	(4/3)
1	2	3	4	5
0	.48	.45	+.03	+.0667
5	.50	.43	+.07	+.1630
10	.50	.41	+.09	+.2190
15	.50	.39	+.11	+.2820
20	.49	.37	+.12	+.3240
25	.47	.32	+.15	+.4680
30	.42	.30	+.12	+.4000
35	.35	.27	+.08	+.2960
40	.29	.25	+.04	+.1600
45	.23	.22	+.01	+.0455
50	.18	.20	-.02	-.1000
55	.14	.17	-.03	-.1760
60	.10	.15	-.05	-.3330

$\sum \frac{\Delta x P_i}{DW_i} = 2.4242$, and $\sum \frac{\Delta x n_i}{DW_i} = 0.6090$

Therefore, $\sum \frac{\Delta x_i}{DW_i} = 2.4242 + 0.6090 = 3.0332$

$C_a = 1.0 - (2.4242 - 0.6090) = 1.0 - (1.8152) = 0.8615$

$C_p = 1.0 - (3.0332) = 1.0 - 0.233 = 0.767$

CHAPTER V

RESULTS AND DISCUSSION

The results obtained from simulation utilizing the two computer programs, Tables 2 (p. 19-22) and 3 (p. 27-28), will be discussed separately. Although infiltration through the surface may be considered to be a special case of infiltration from a buried source, the former process is important in itself because of its influence in many natural as well as artificially induced hydrologic events.

Infiltration through the Surface

The results of simulation on the three soils, Yolo light clay, Adelanto loam, and Pachappa loam, are presented in Figures 11 through 18 in the form of water content profiles with time, average infiltration rates with time, and cumulative amounts of infiltration with time. The results from Yolo light clay provided a comparison with the solution obtained for identical boundary and initial conditions by Philip (1957a, 1957b), whereas those for Adelanto and Pachappa loam demonstrated the workability of the method for soils having different hydraulic characteristics (Bhuiyan et al., 1971).

Comparison between results obtained for Yolo light clay by simulation and Philip's method, as illustrated in Figures 11, 15, and 17, shows fairly good agreement. It is evident, however, that CSMP solution yields water content profiles which penetrate to a greater

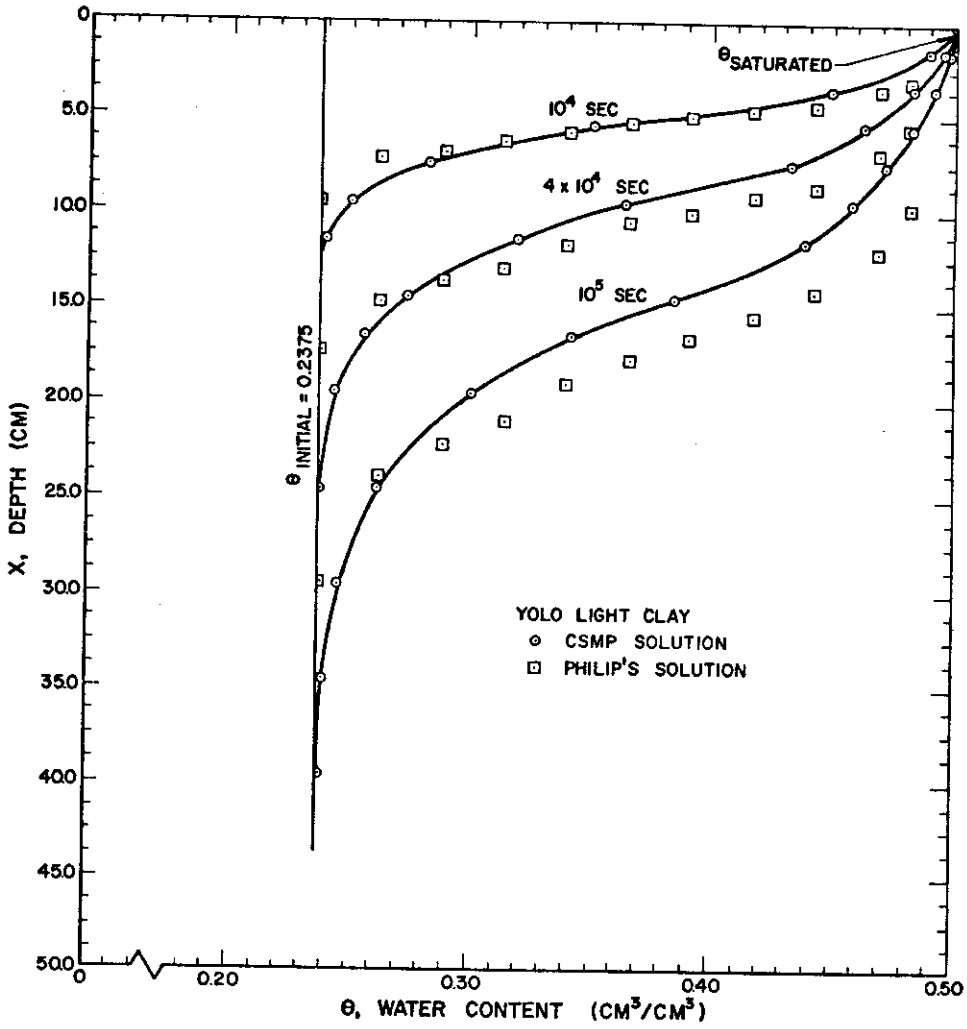

Figure 11 Water content profiles for vertical infiltration through surface into unsaturated Yolo light clay with initial uniform pressure potential of -660.0 cm of water

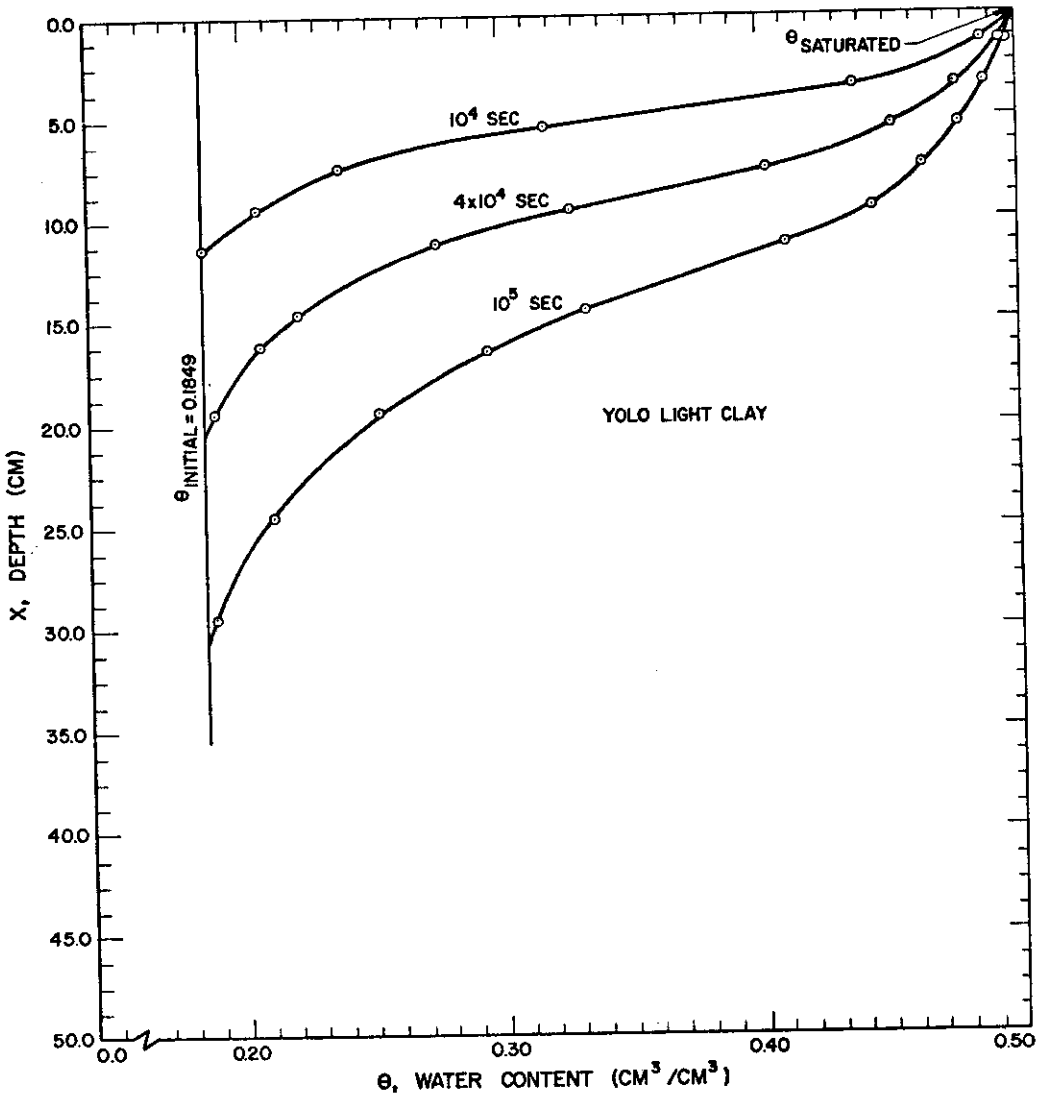

Figure 12 Water content profiles for vertical infiltration through surface into unsaturated Yolo light clay with initial uniform pressure potential of -2000.0 cm of water

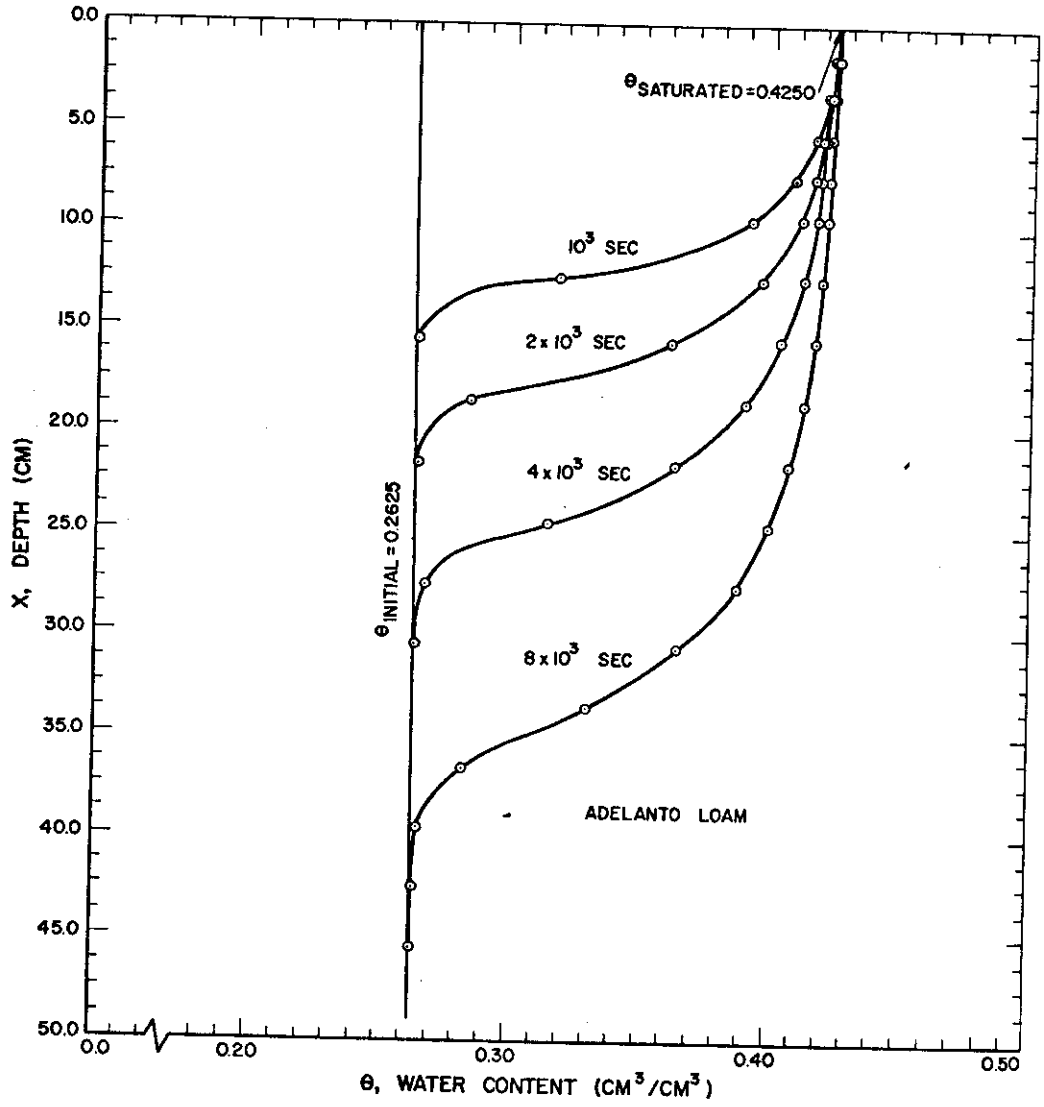

Figure 13 Water content profiles for vertical infiltration through surface into unsaturated Adelanto loam with initial uniform pressure potential of -660.0 cm of water

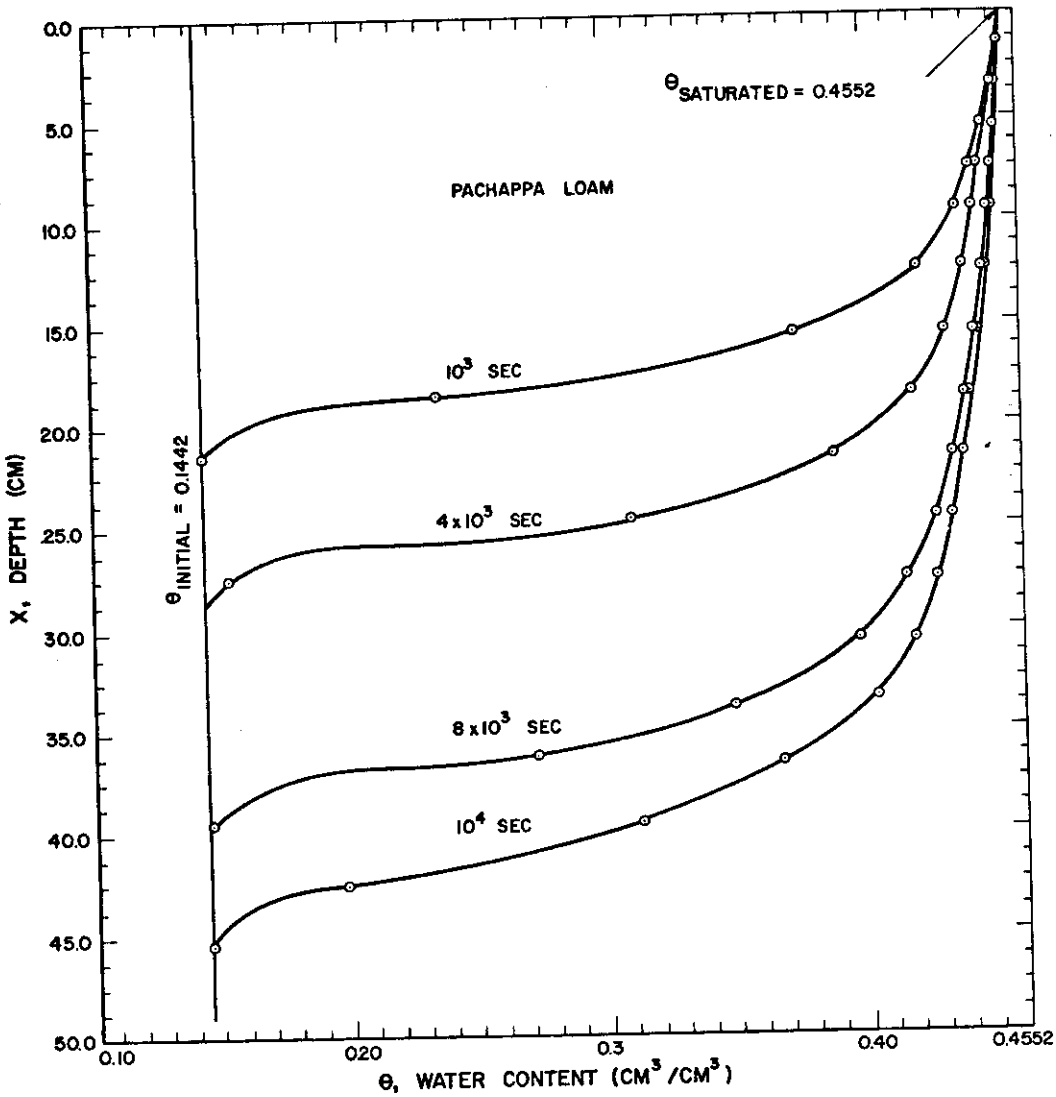

Figure 14 Water content profiles for vertical infiltration through surface into unsaturated Pachappa loam with initial uniform pressure potential of -660.0 cm of water

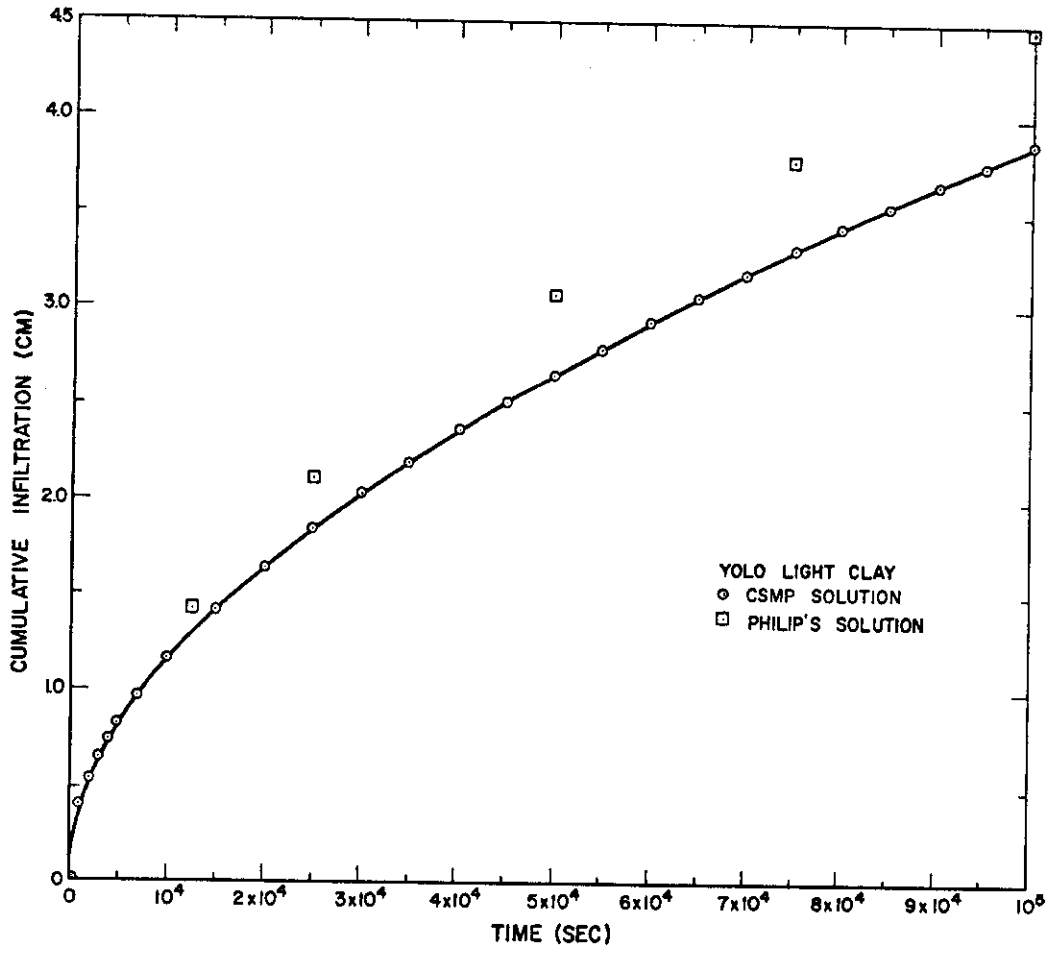

Figure 15 Cumulative infiltration amount with time for Yolo light clay with initial uniform pressure potential of -660.0 cm of water

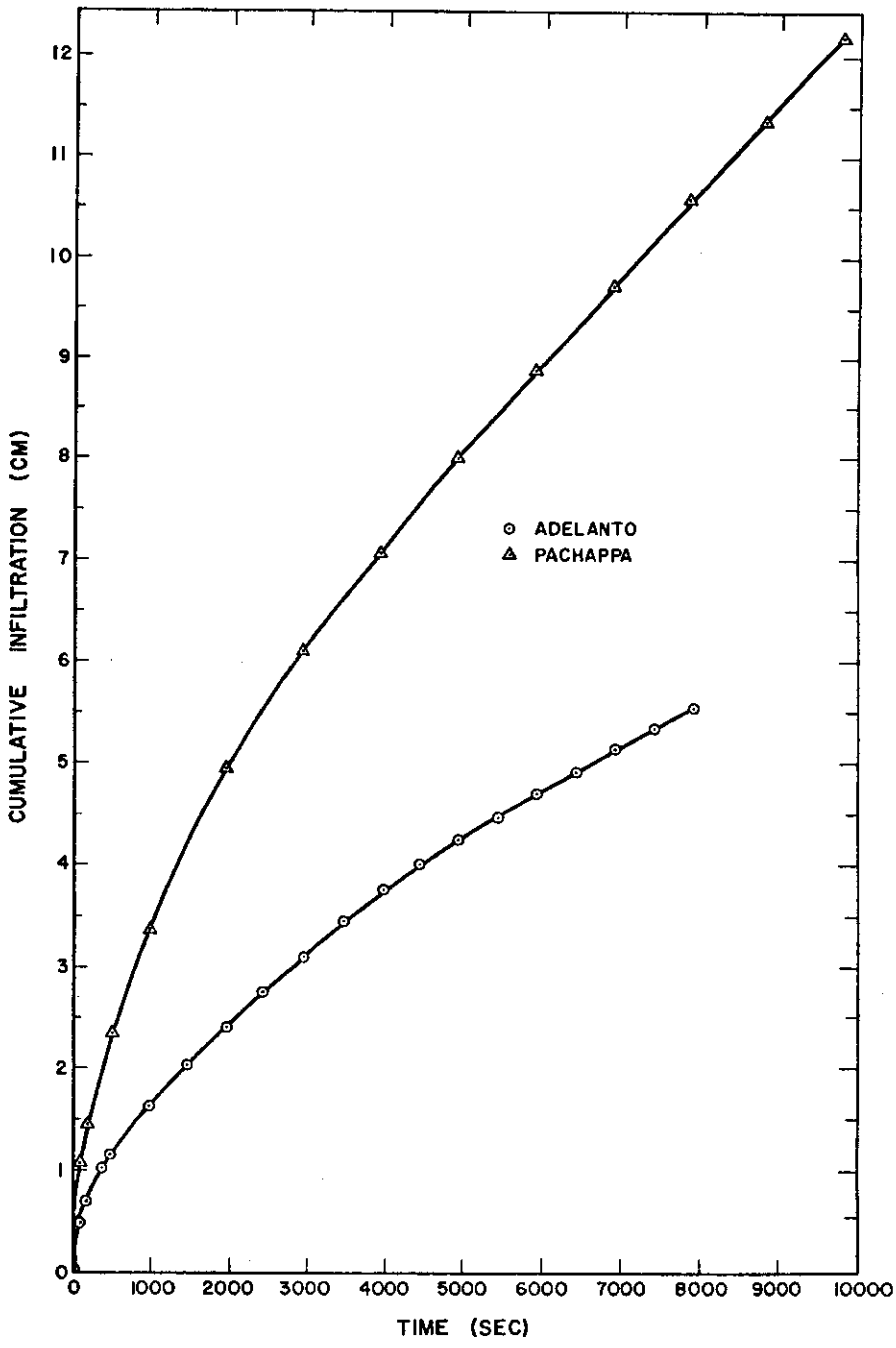

Figure 16 Cumulative infiltration amount with time for Adelanto and Pachappa loam with initial uniform pressure potential of -660.0 cm of water

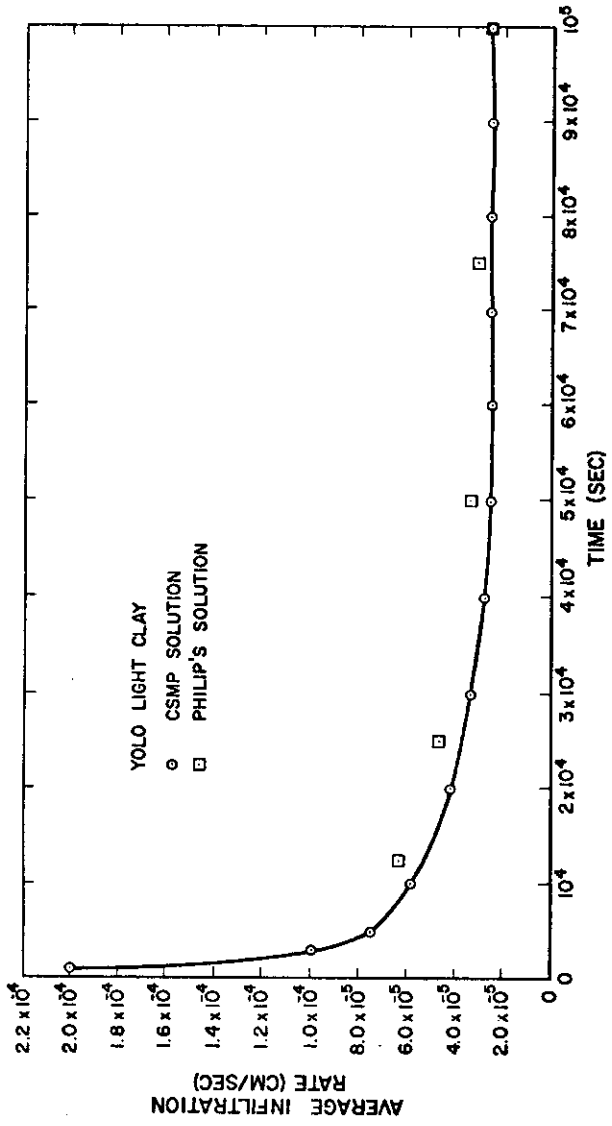

Figure 17 Average infiltration rate with time for Yolo light clay with initial uniform pressure potential of -660.0 cm of water

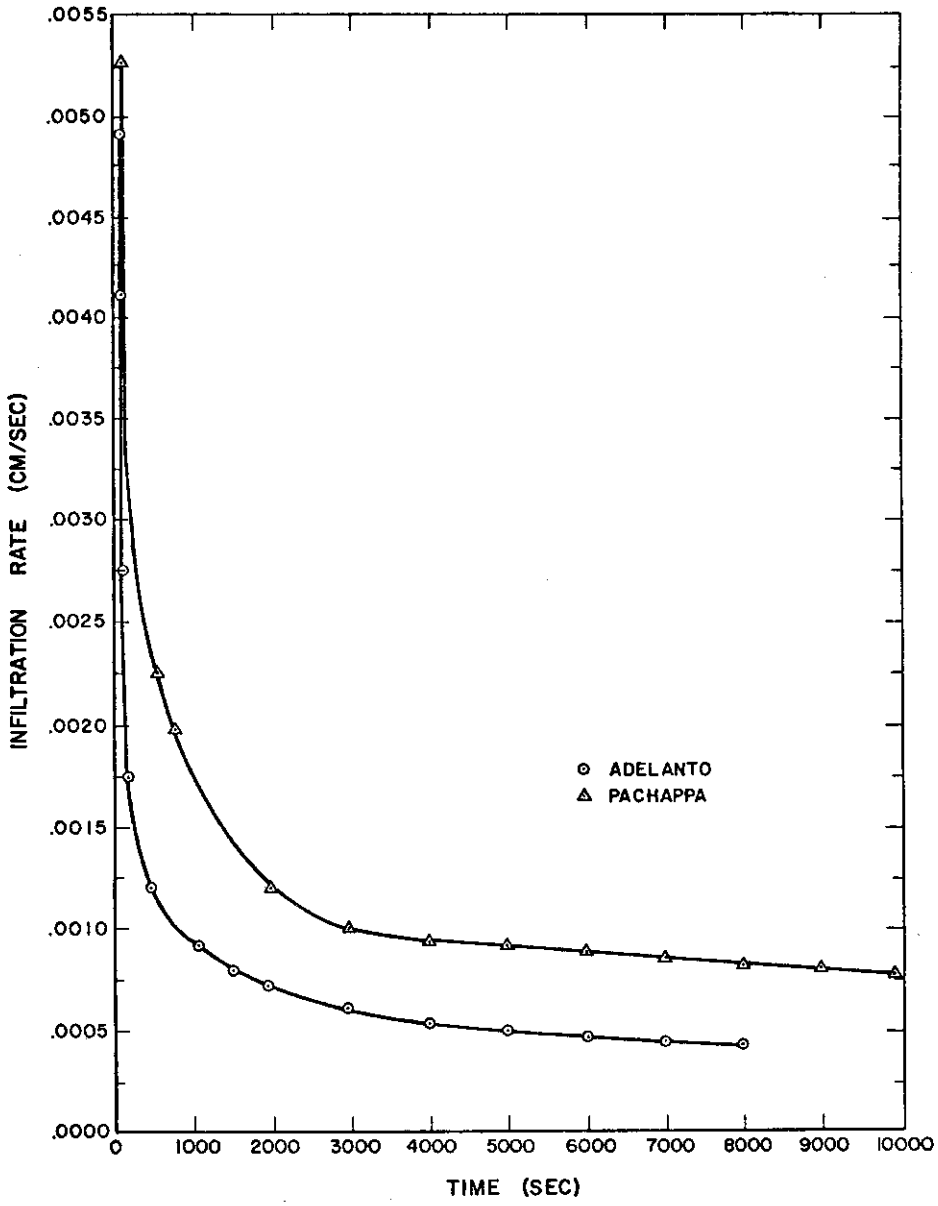

Figure 18 Average infiltration rate with time for Adelanto and Pachappa loam with initial uniform pressure potential of -660.0 cm of water

depth for a given time and have a less abrupt end to the profiles. The hydraulic properties of Yolo light clay used in this work were read from the curves presented by Philip (1969). To make them usable for the purpose of the comparison, the water content vs. conductivity curve shown by Philip had to be extrapolated and, thus, unavoidable errors might have been introduced into the input values of the CSMP model. However, it is interesting to note that a comparison of water content profiles obtained in field experiments and calculated by Philip's method (Nielsen et al., 1961) showed a similar comparison to that illustrated in Figure 11.

Figure 12 (p. 44) demonstrates the effect of a lower initial pressure potential, -2000.0 cm of water, on the water content profiles. Although the wetting front penetrated less deeply, the total amount of infiltration, as calculated by the program, was higher in this case than that in the case of Figure 11 (p. 43). The total infiltration amounts were 4.37 cm and 3.84 cm, respectively.

The infiltration process was more rapid in Adelanto and Pachappa soils than in Yolo light clay, as one would expect from their hydraulic properties. The infiltration rates calculated by the model were the instantaneous values and were highly variable. Therefore, average infiltration rates for each soil, as shown in Figures 17 (p. 49) and 18 (p. 50), were obtained by measuring the slopes from the appropriate cumulative infiltration curves.

The error in integration for solutions in Yolo light clay was specified to be equal to, or less than, 0.1 percent, which meant a

very high degree of accuracy. In the case of the other two soils, the error limit was increased to 10 percent in order to reduce the required computer time. The more hydraulically conductive the soil is, the smaller are the integration steps to meet a given error bound. Thus, in case of more conductive soils, the total number of iterations to reach a given time solution becomes very large in comparison to what is necessary for a less conductive soil.

Infiltration from Buried Sources and Redistribution

The water content profiles, presented in Figures 19 through 32, illustrate how water is distributed in time and space during infiltration from buried sources and, subsequently, redistributed through the drying cycle. Tables 5 and 6 summarize the main aspects of the simulated data.

Let us consider the results of simulation for the source at 30-cm depth and initial water content of 0.2375 (cm^3/cm^3). When the control point is located four centimeters above the center of the source, as shown in Figure 24, there is no infiltration above layer 21 and below layer 41. The root consumption rate being the highest in the top of the root zone, the drying cycle profile at the end of 11.0 hours shows considerable depletion of water from the initial value in that part. This depletion is avoided in Figures 25, 26, and 27 where the control points are further away from the source compared to the previous case. There are, however, two other interesting developments that become evident in these figures. First, depletion

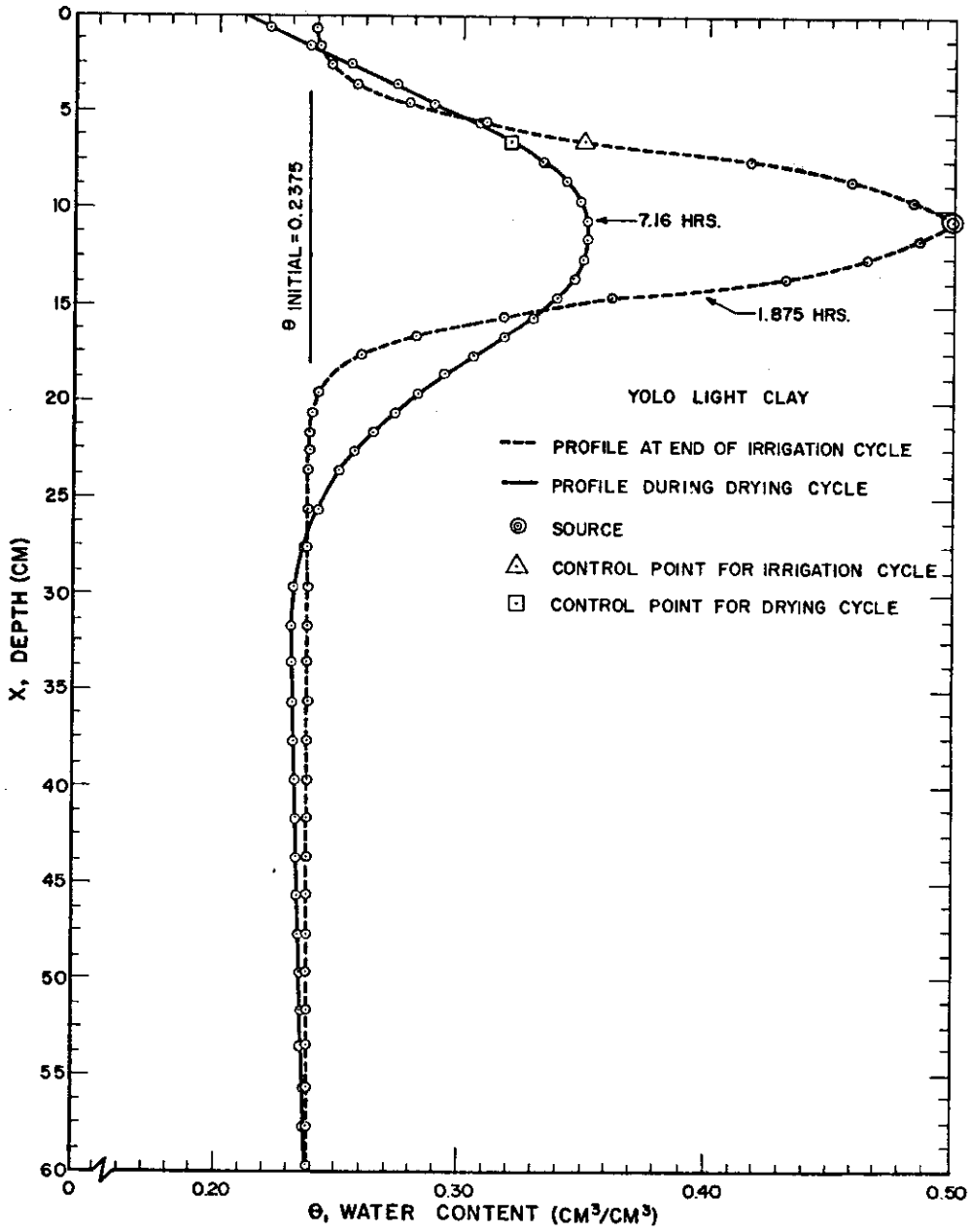

Figure 19 Water content profiles during infiltration and drying cycles with initial uniform water content of 0.2375 (cm^3/cm^3), source at 10.0 cm depth and control points at 4.0 cm above center of source

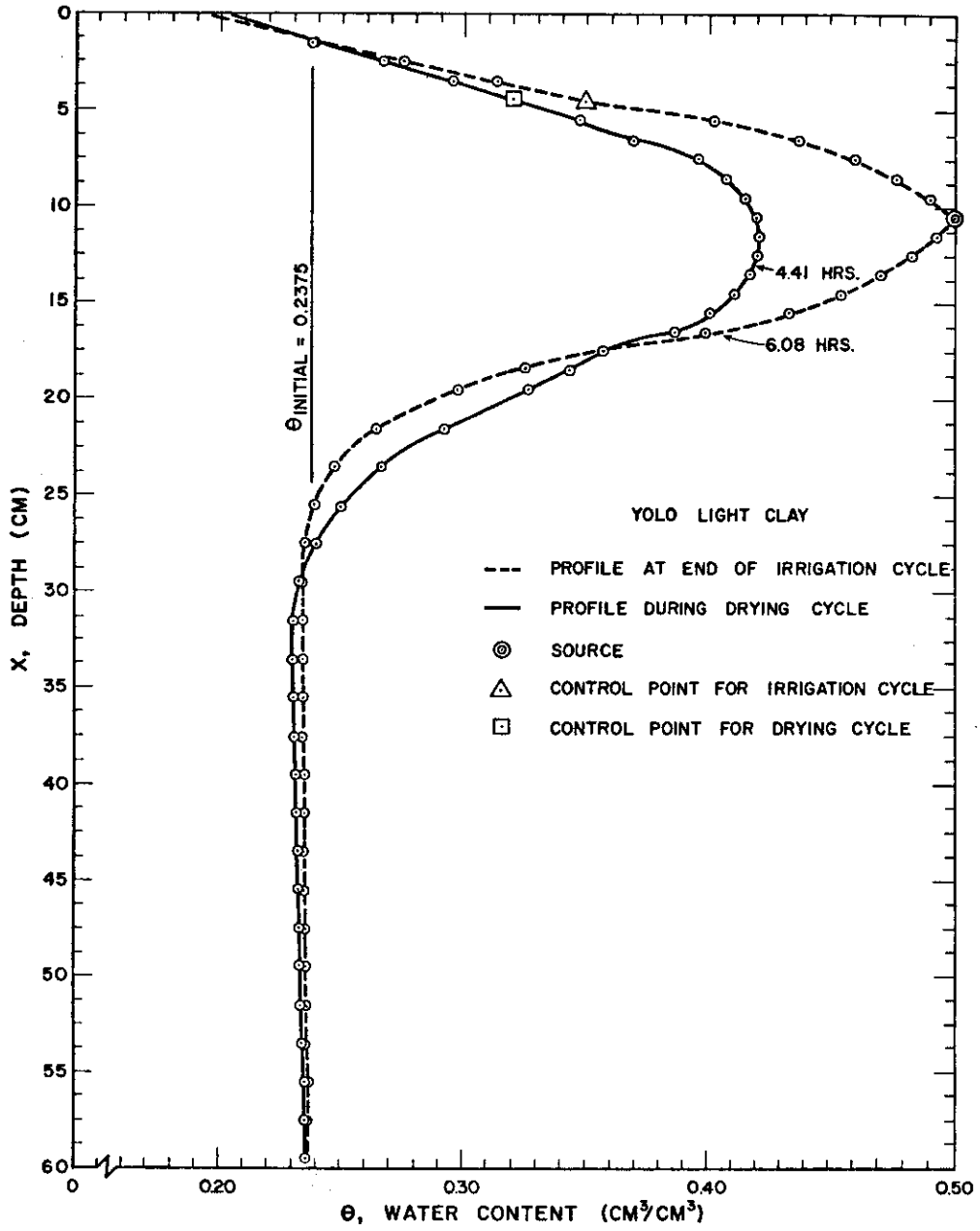

Figure 20 Water content profiles during infiltration and drying cycles with initial uniform water content of 0.2375 (cm^3/cm^3), source at 10.0 cm depth and control points at 6.0 cm above center of source

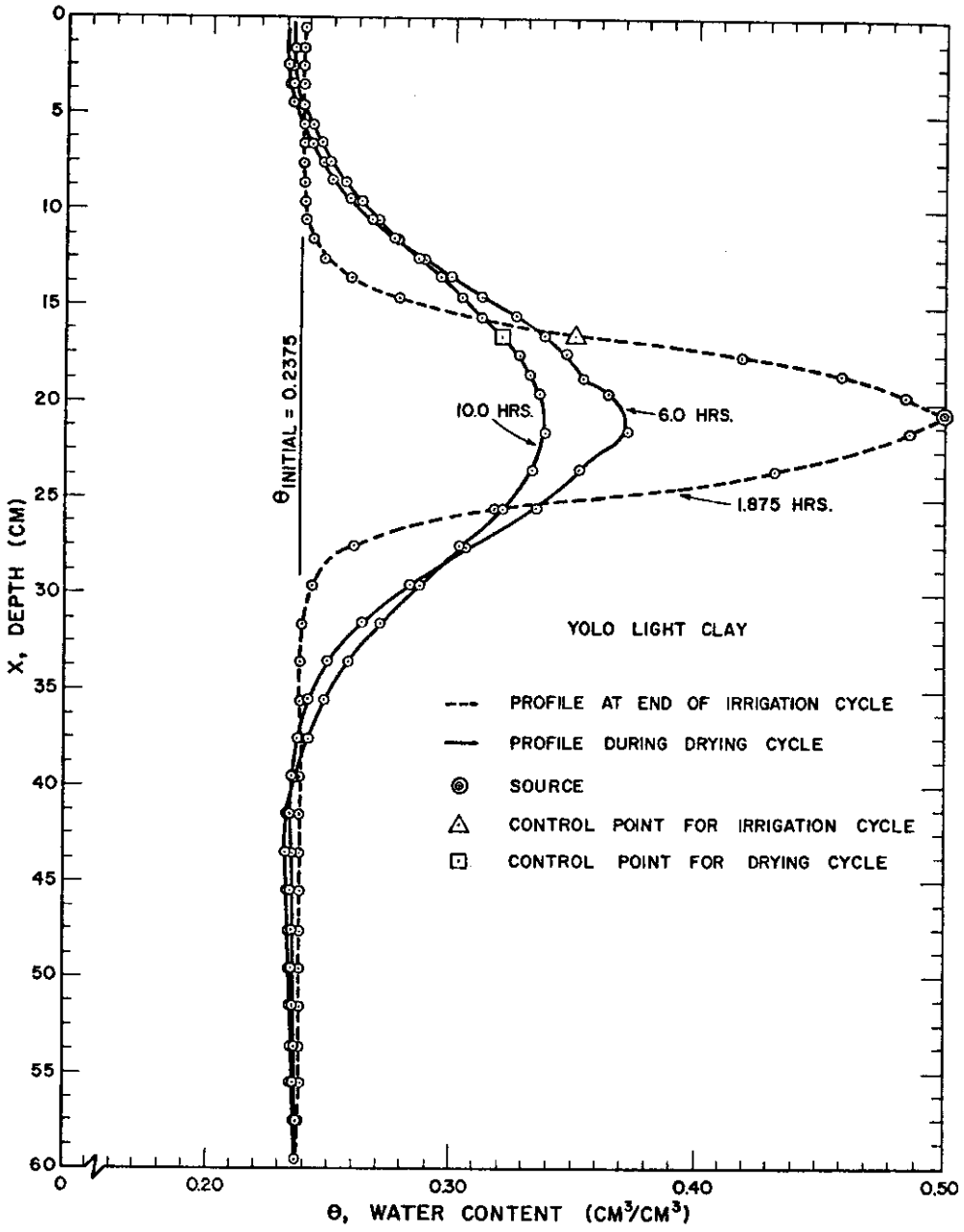

Figure 21 Water content profiles during infiltration and drying cycles with initial uniform water content of 0.2375 (cm^3/cm^3), source at 20.0 cm depth and control points at 4.0 cm above center of source

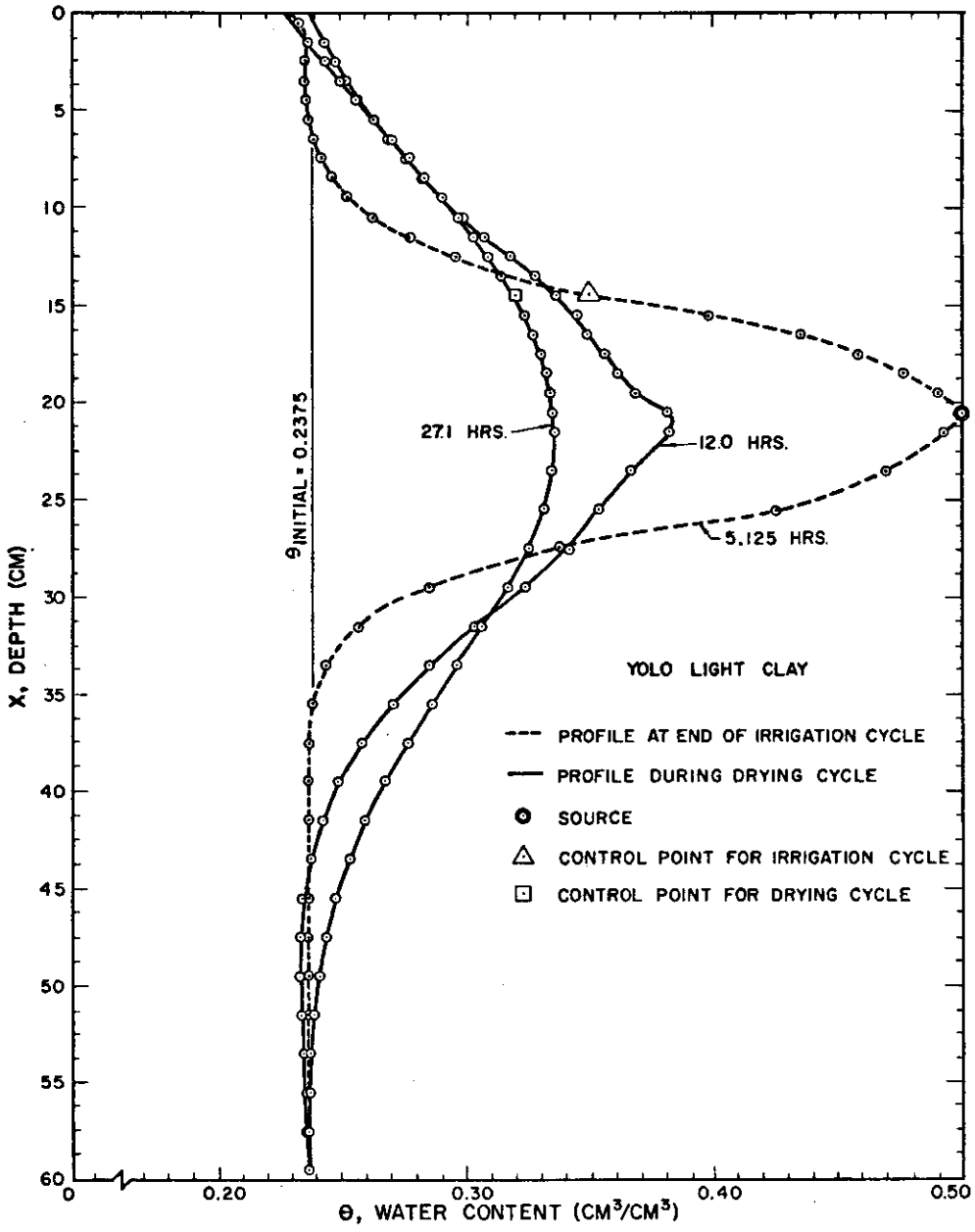

Figure 22 Water content profiles during infiltration and drying cycles with initial uniform water content of 0.2375 (cm^3/cm^3), source at 20.0 cm depth and control points at 6.0 cm above center of source

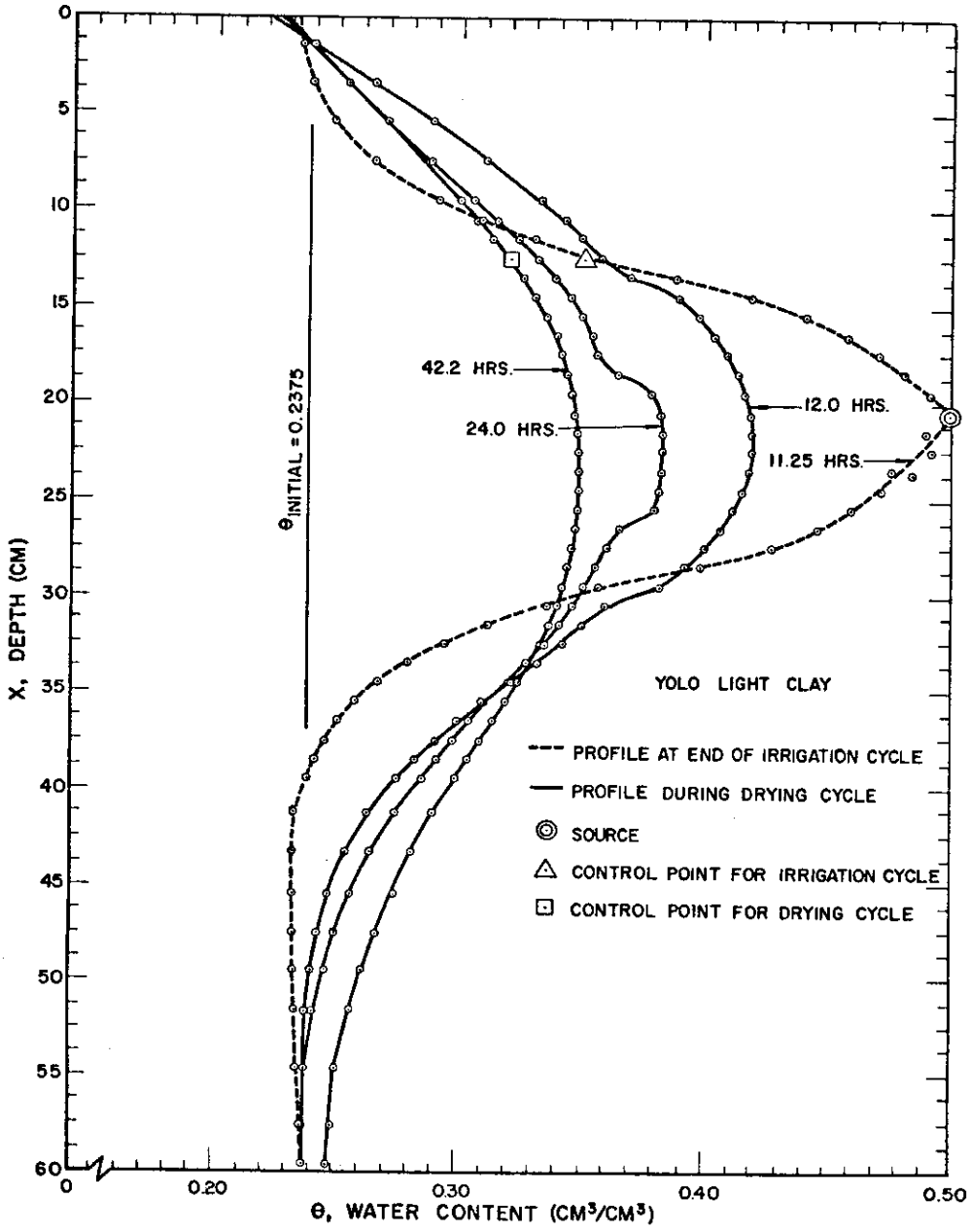

Figure 23 Water content profiles during infiltration and drying cycles with initial uniform water content of 0.2375 (cm^3/cm^3), source at 20.0 cm depth and control points at 8.0 cm above center of source

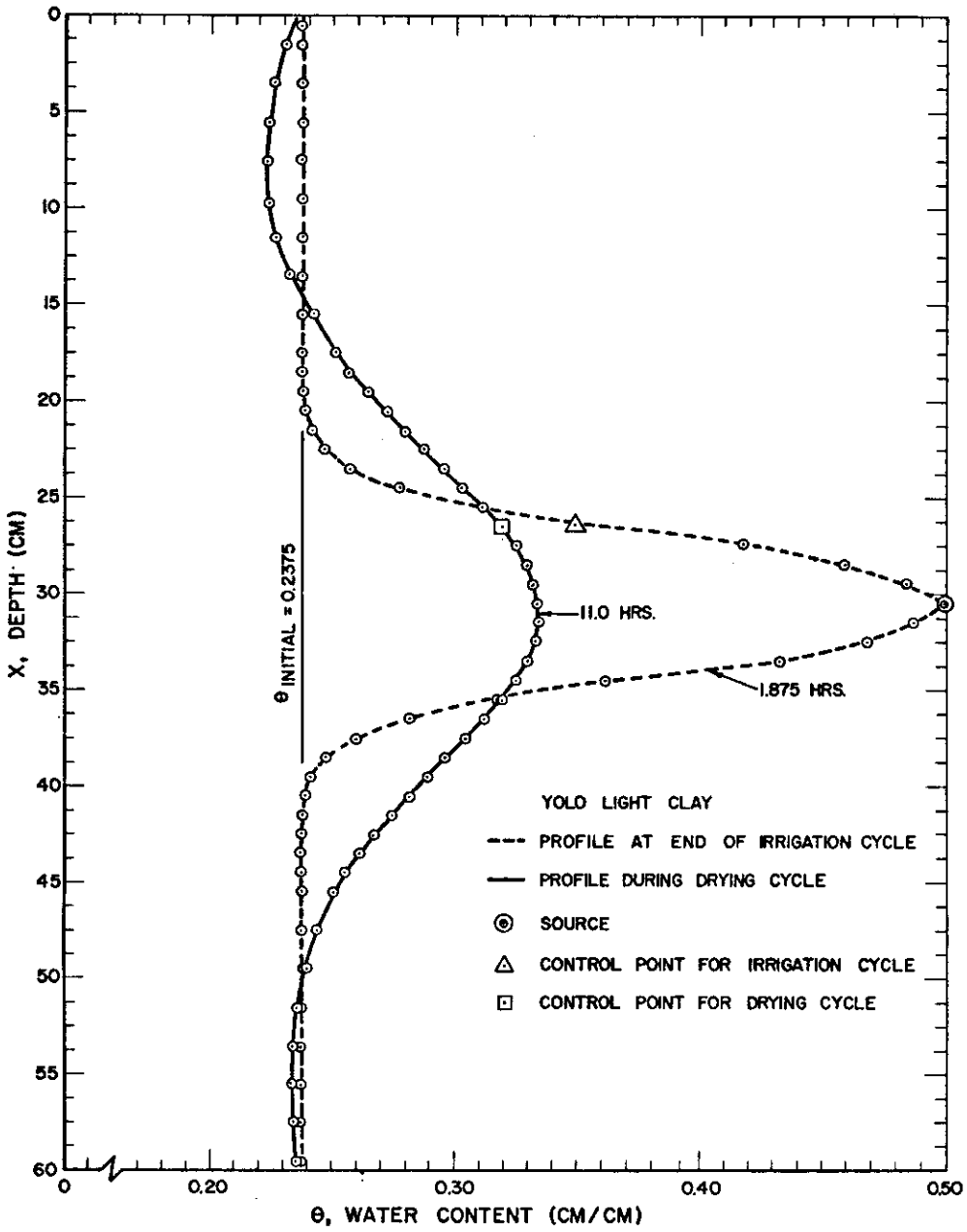

Figure 24 Water content profiles during infiltration and drying cycles with initial uniform water content of 0.2375 (cm^3/cm^3), source at 30.0 cm depth and control points at 4.0 cm above center of source

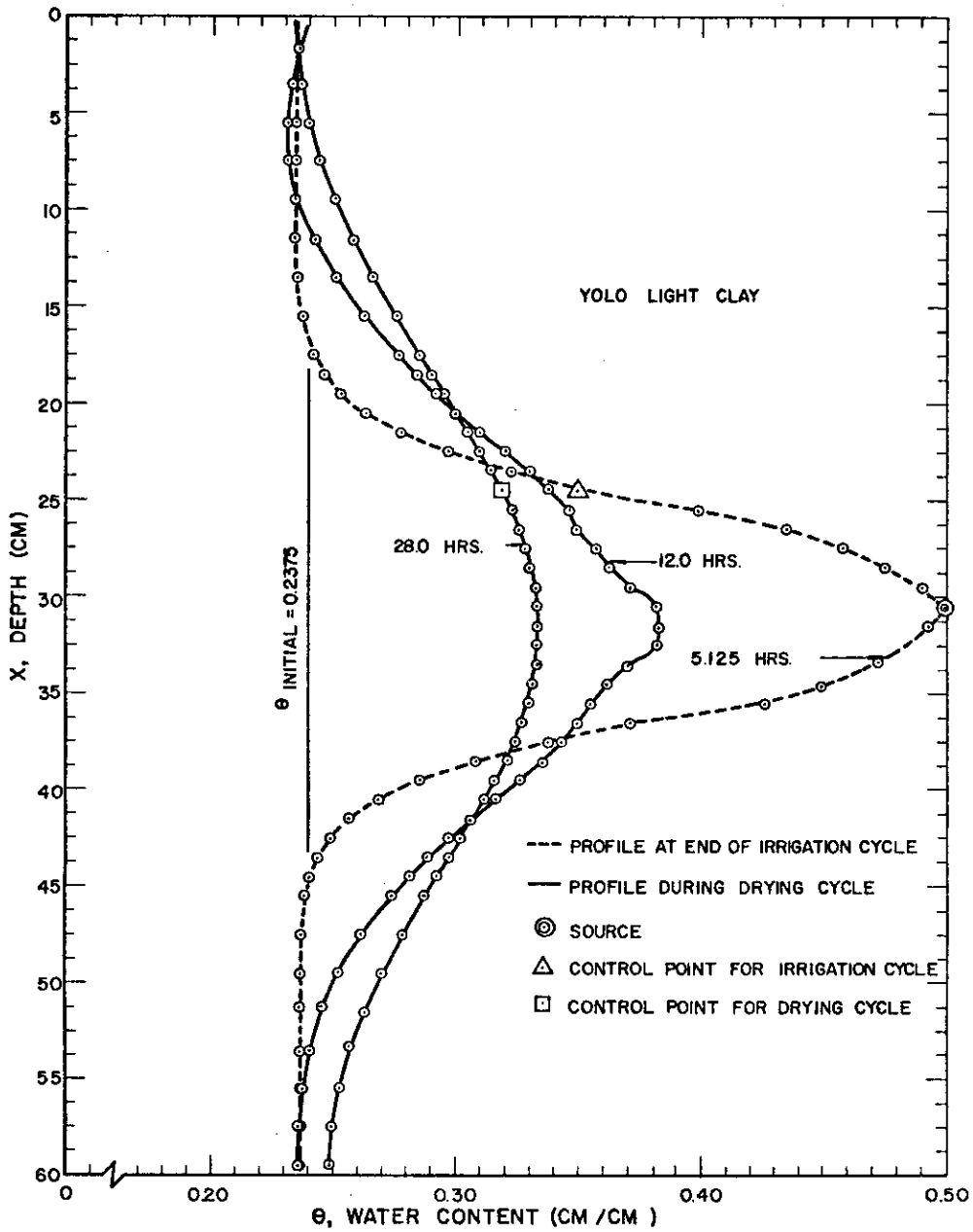

Figure 25 Water content profiles during infiltration and drying cycles with initial uniform water content of 0.2375 (cm^3/cm^3), source at 30.0 cm depth and control points at 6.0 cm above center of source

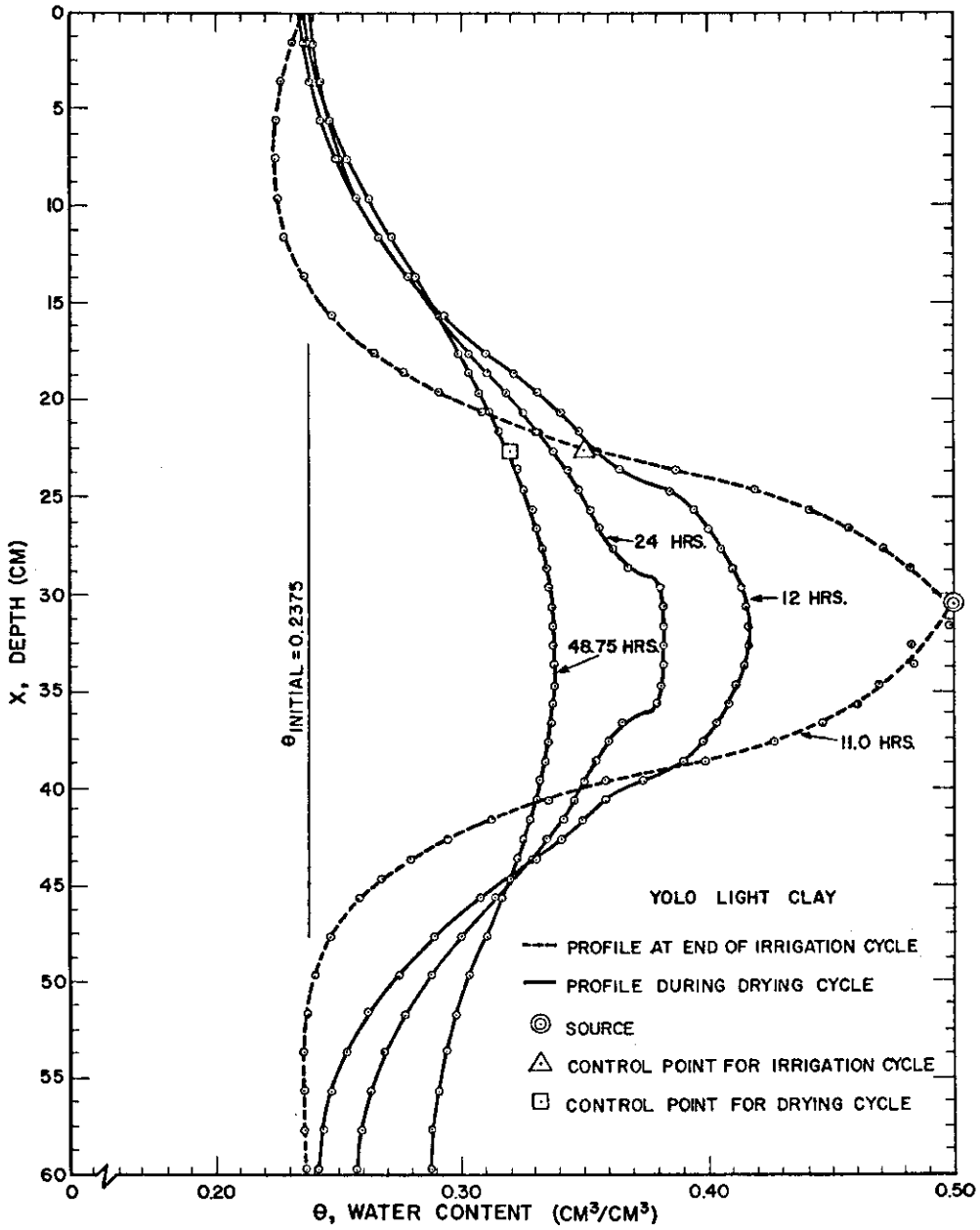

Figure 26 Water content profiles during infiltration and drying cycles with initial uniform water content of 0.2375 (cm^3/cm^3), source at 30.0 cm depth and control points at 8.0 cm above center of source

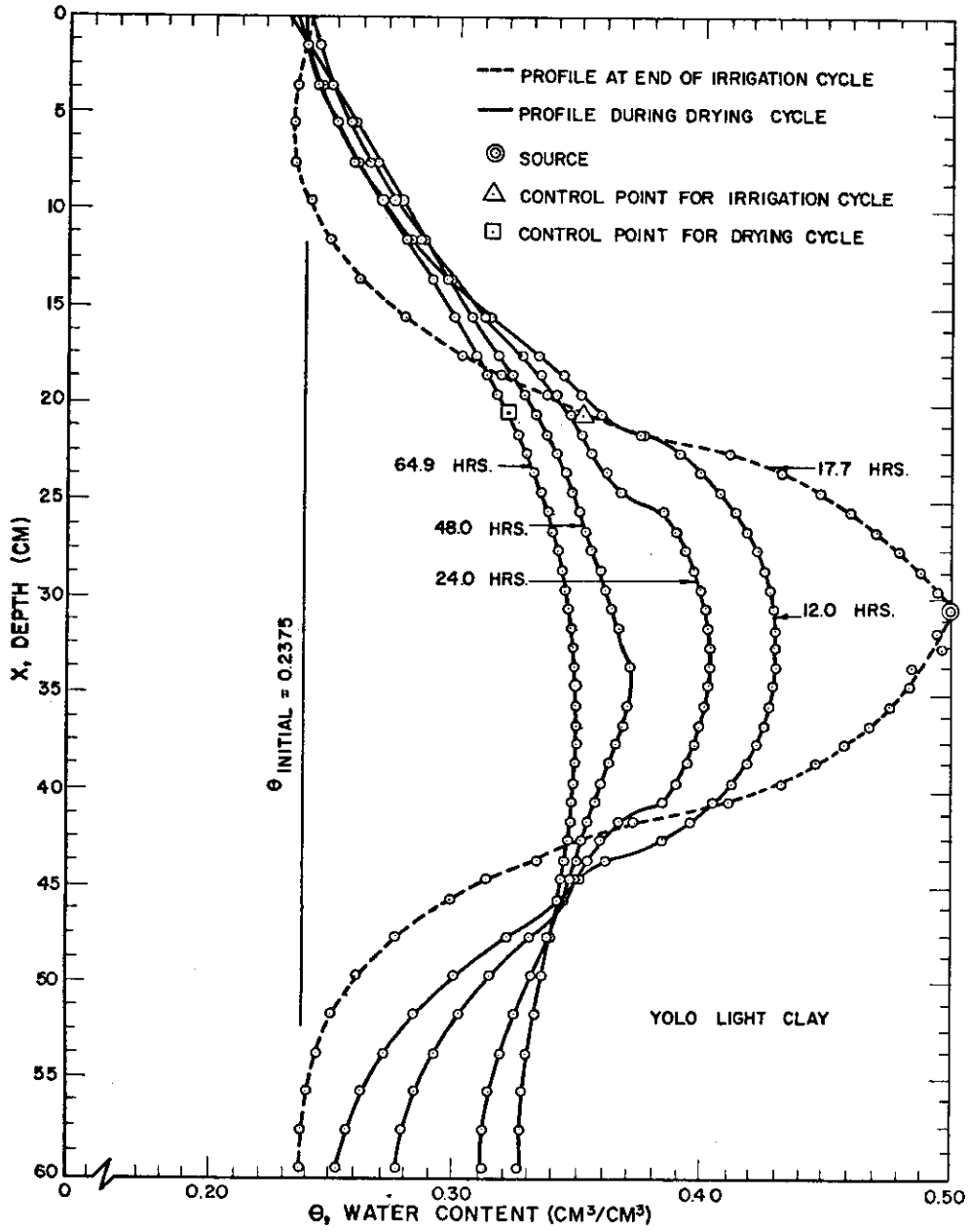

Figure 27 Water content profiles during infiltration and drying cycles with initial uniform water content of 0.2375 (cm^3/cm^3), source at 30.0 cm depth and control points at 10.0 cm above center of source

Table 5 Summary of pertinent results of computer simulation with initial uniform water content of 0.2375 (cm^3/cm^3)

Source	Location (cm below surface) of		Duration of irrigation cycle	Total amount infiltrated	Duration of drying cycle
	control point for irrigation cycle*	control point for drying cycle**	(hours)	(cm)	(hours)
10	6.5(Fig. 19)	6.5	1.875	1.872	7.16
10	4.5(Fig. 20)	4.5	6.080	3.326	4.41
20	16.5(Fig. 21)	16.5	1.875	1.872	10.00
20	14.5(Fig. 22)	14.5	5.125	3.040	27.10
20	12.5(Fig. 23)	12.5	11.250	4.567	42.20
30	26.5(Fig. 24)	26.5	1.875	1.872	11.00
30	24.5(Fig. 25)	24.5	5.125	3.041	28.00
30	22.5(Fig. 26)	22.5	11.000	4.498	48.75
30	20.5(Fig. 27)	20.5	17.700	5.744	64.90

* Cut-off water content value at the control point for irrigation cycle = 0.35 (cm^3/cm^3)

** Cut-off water content value at the control point for drying cycle = 0.32 (cm^3/cm^3)

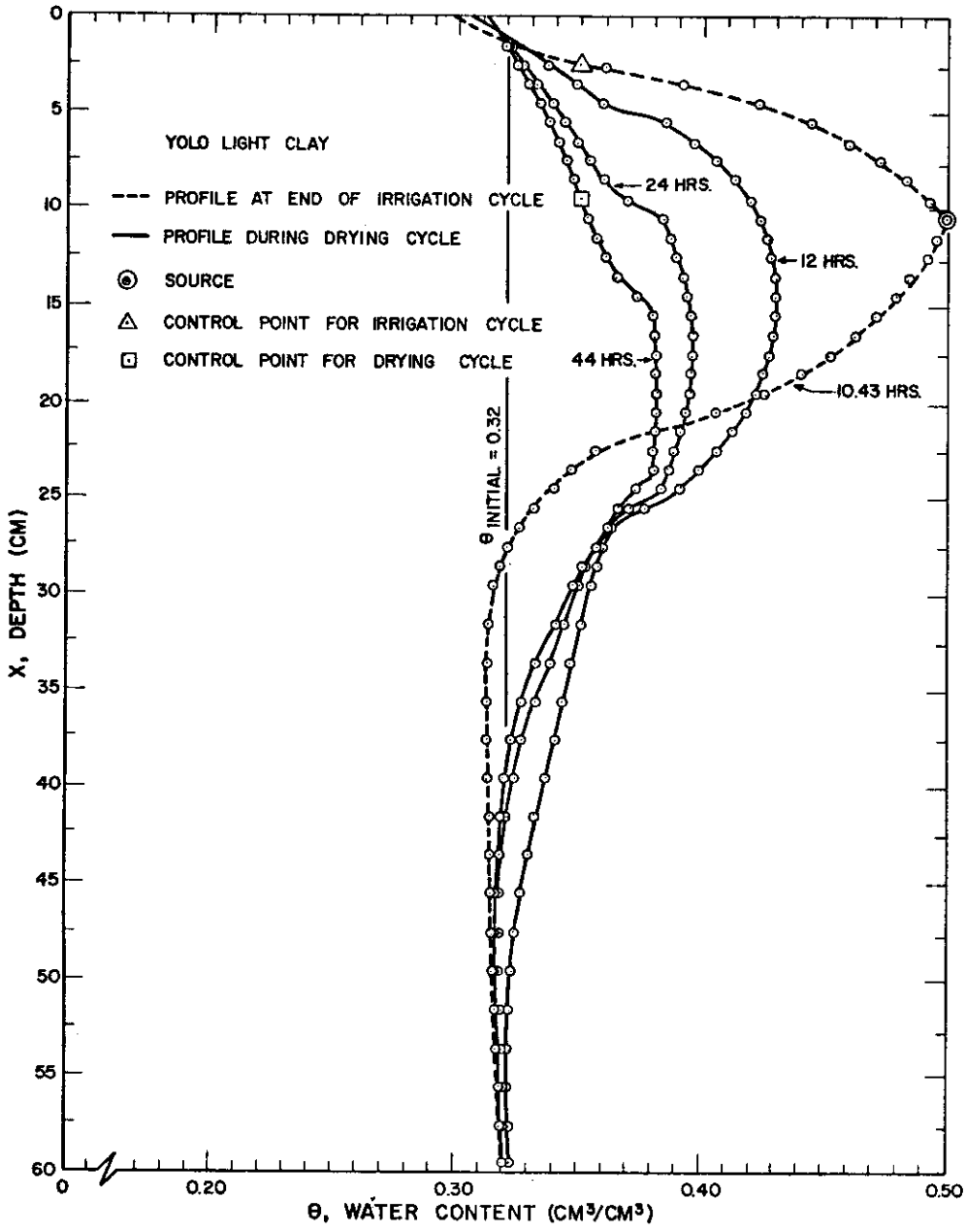

Figure 28 Water content profiles during infiltration and drying cycles with initial uniform water content of 0.32 (cm^3/cm^3), source at 10.0 cm depth and irrigation and drying cycle control points at 8.0 cm and 1.0 cm, respectively, above center of source

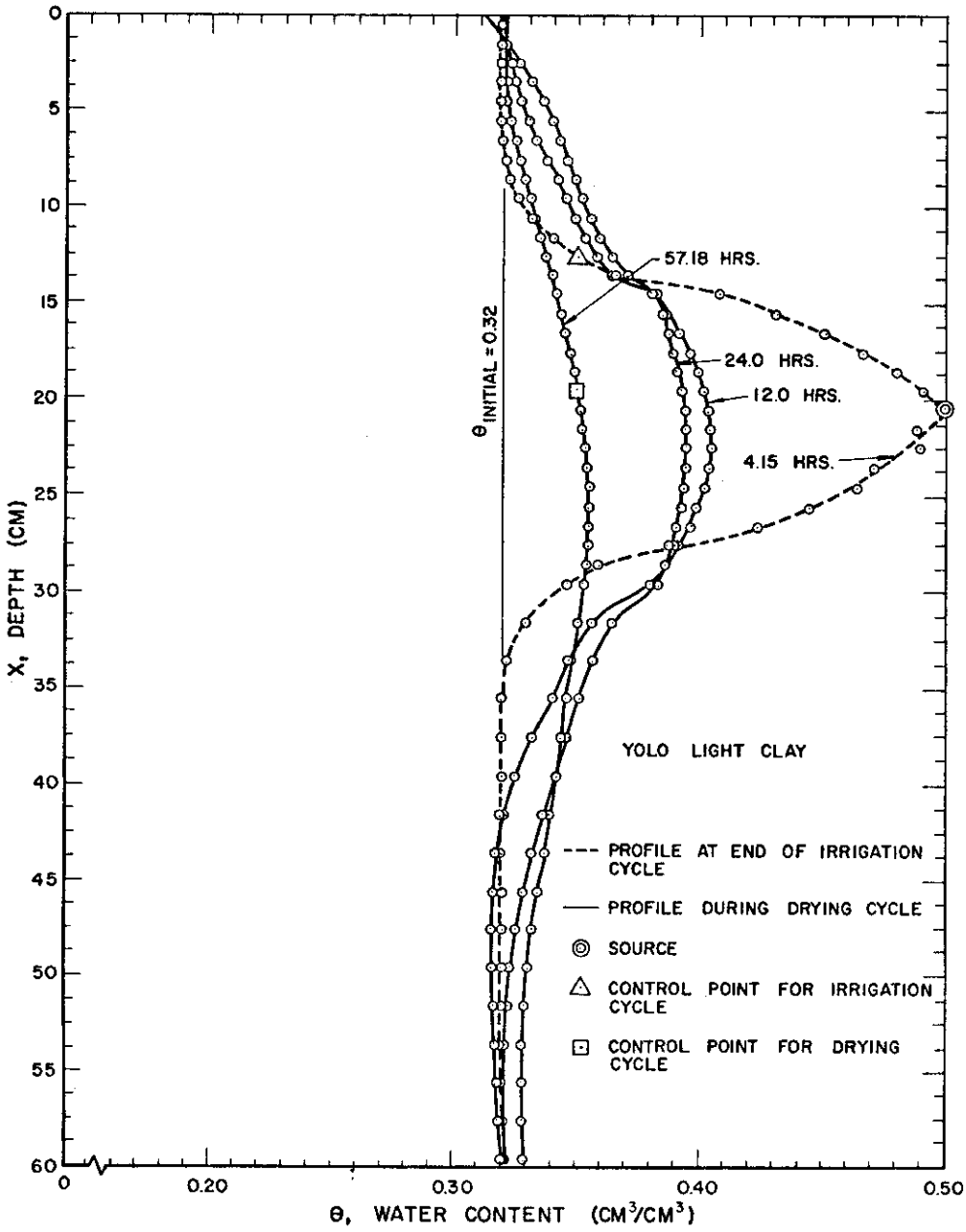

Figure 29 Water content profiles during infiltration and drying cycles with initial uniform water content of 0.32 (cm^3/cm^3), source at 20.0 cm depth and irrigation and drying cycle control points at 8.0 cm and 1.0 cm, respectively, above center of source

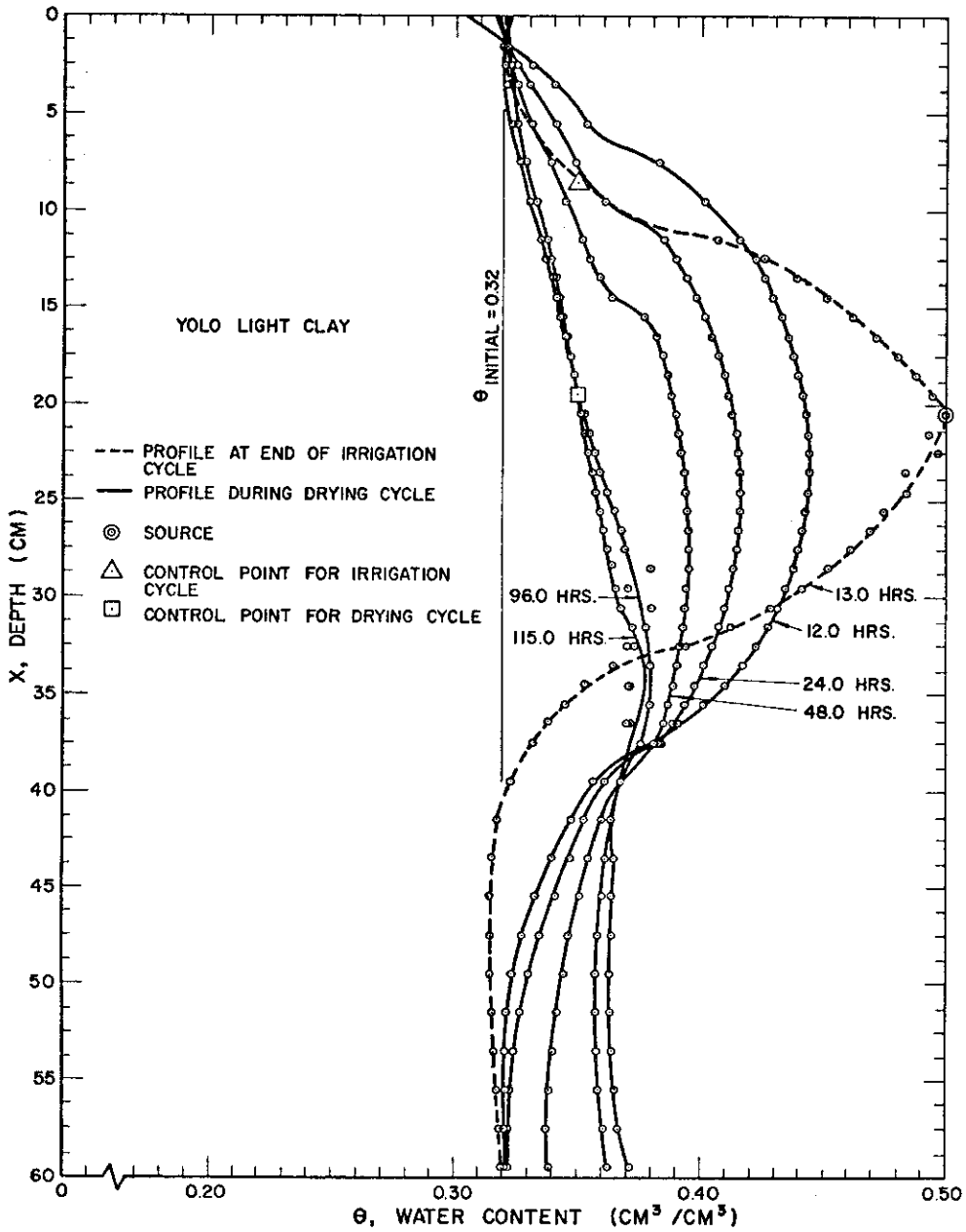

Figure 30 Water content profiles during infiltration and drying cycles with initial uniform water content of 0.32 (cm^3/cm^3), source at 20.0 cm depth and irrigation and drying cycle control points at 12.0 cm and 1.0 cm, respectively, above center of source

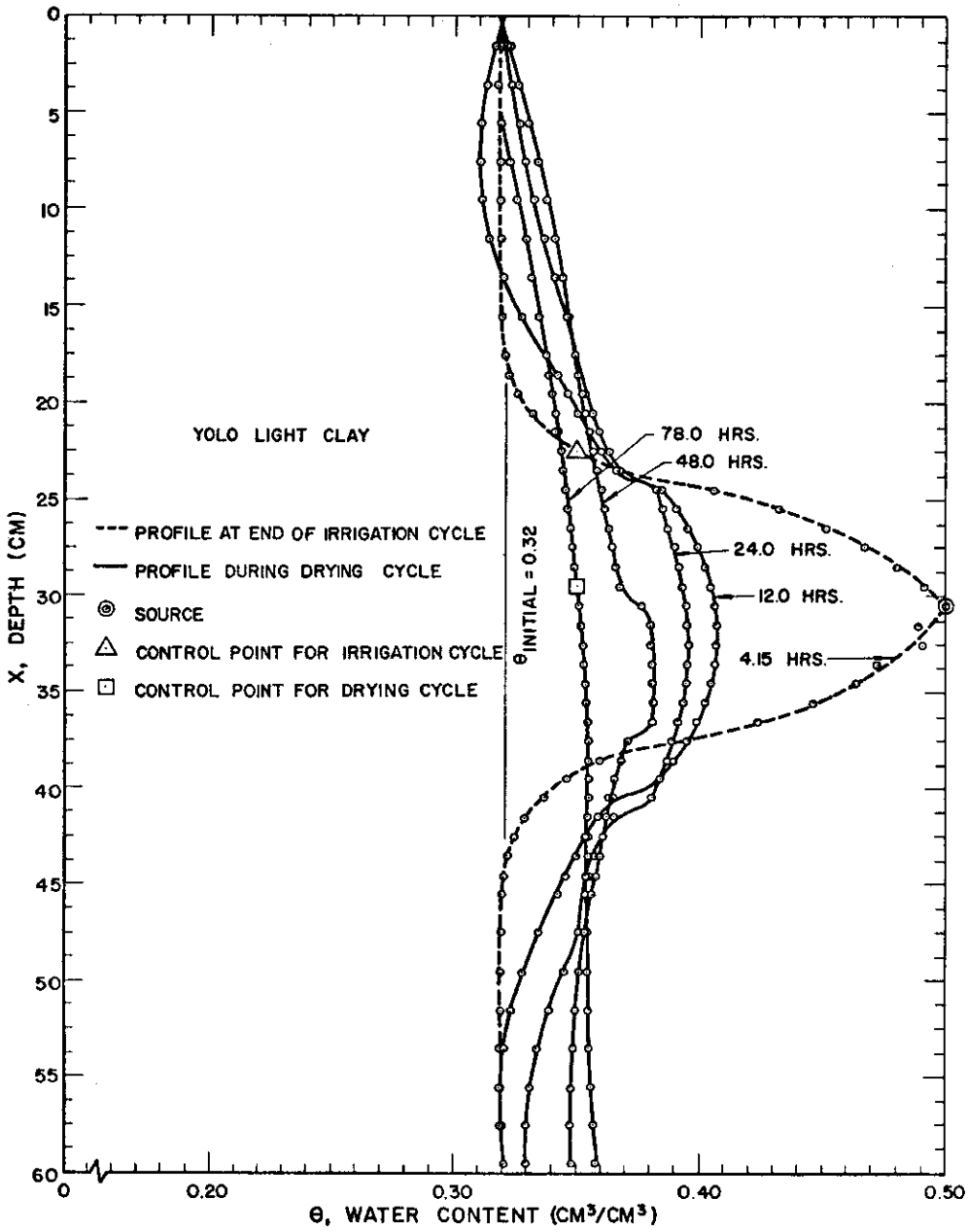

Figure 31 Water content profiles during infiltration and drying cycles with initial uniform water content of 0.32 (cm^3/cm^3), source at 30.0 cm depth and irrigation and drying cycle control points at 8.0 cm and 1.0 cm, respectively, above center of source

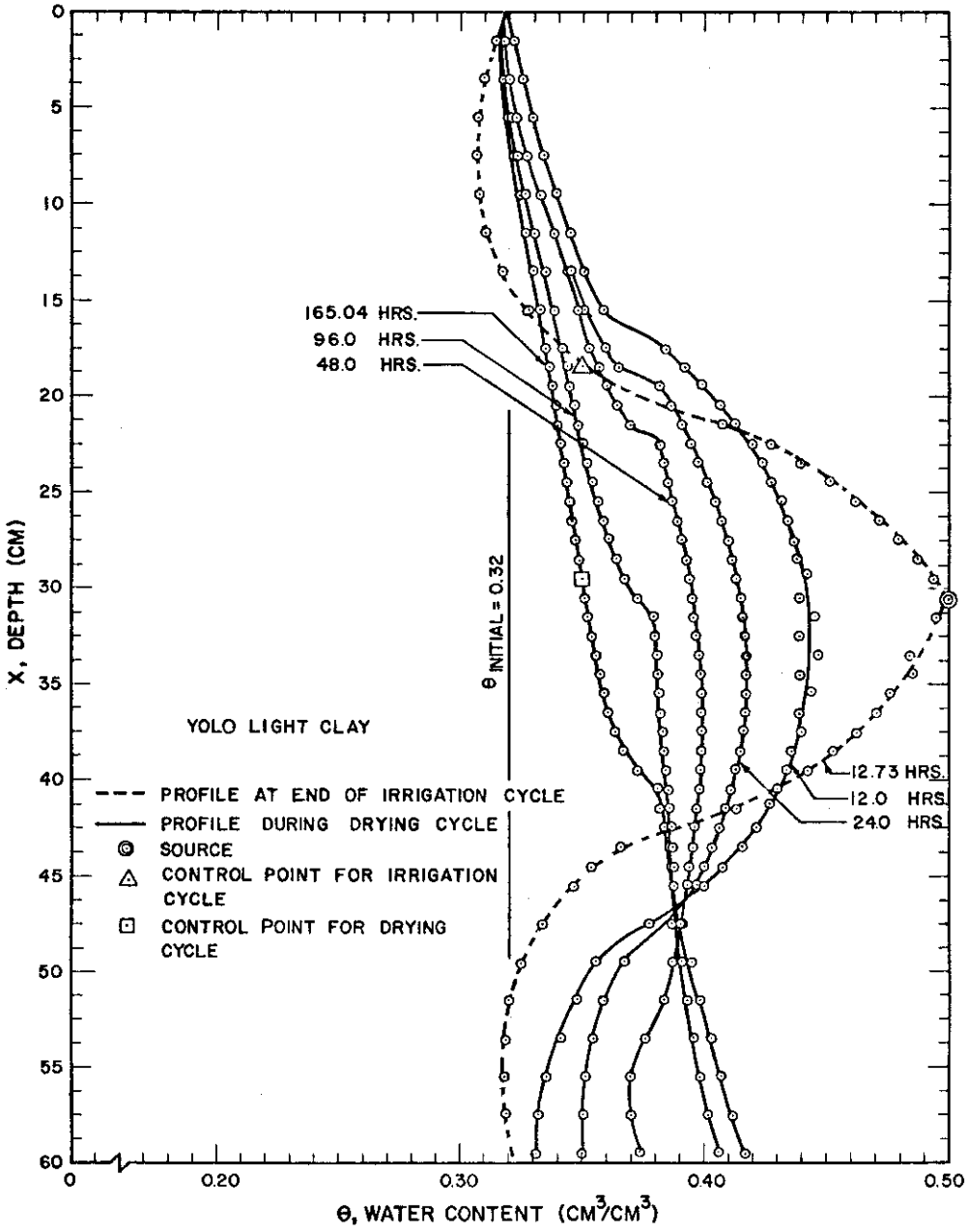

Figure 32 Water content profiles during infiltration and drying cycles with initial uniform water content of 0.32 (cm^3/cm^3), source at 30.0 cm depth and irrigation and drying cycle control points at 12.0 cm and 1.0 cm, respectively, above center of source

Table 6 Summary of pertinent results of computer simulation with initial uniform water content of 0.32 (cm^3/cm^3)

Source	Location (cm below surface) of		Duration of irrigation cycle	Total amount infiltrated	Duration of drying cycle
	control point for irrigation cycle*	control point for drying cycle**	(hours)	(cm)	(hours)
10	2.5(Fig. 28)	9.5	10.43	3.365	44.00
20	12.5(Fig. 29)	19.5	4.15	2.003	57.18
20	8.5(Fig. 30)	19.5	13.00	3.739	115.00
30	22.5(Fig. 31)	29.5	4.15	2.002	78.00
30	18.5(Fig. 32)	29.5	12.73	3.658	165.04

* Cut-off water content value at the control point for irrigation cycle = 0.35 (cm^3/cm^3)

** Cut-off water content value at the control point for drying cycle = 0.35 (cm^3/cm^3)

from initial water content occurs during the irrigation cycle. Second, accumulation of water at the bottom increases in proportion to the distance of the control point from the source. If the irrigation cycle is continued for a long time, or after several irrigation cycles, a build-up of water table at the bottom can be expected. Identical results also are obtained with initial uniform water content of 0.32 (cm^3/cm^3), as shown in Figures 31 (p. 66) and 32 (p. 67), although they have different locations and cut-off water content values of the control points. It is evident that an excessive accumulation of water at the bottom will result in low values of the availability and proportionality coefficients and create poor water-use efficiency, since this water will not likely be utilized by the plant.

The simulation results for the source at 20 cm depth illustrate a similar trend. With the drier initial water content and control point four centimeters above the center of the source, as shown in Figure 21 (p. 55), the top six centimeters and the bottom 22 cm of the root zone deplete water at the end of the drying cycle. In Figure 22 (p. 56), having the control point moved six centimeters above the center of the source, no significant depletion of water from the initial value is evidenced at the end of the drying cycle. But, it is obvious from the pattern of movement of the profiles with time that accumulation at the bottom will start if the drying cycle is continued longer or another set of cycles is performed. In Figure 23 (p. 57), the control point is set further away from the source than

in Figure 22 (p. 56). This resulted in a longer duration for both of the cycles. As a result, depletion from the initial water content at the end of the irrigation cycle and considerable accumulation of water at the bottom at the end of the drying cycle are evident. With the wetter initial condition, the build-up of water at the bottom, as shown in Figures 29 (p. 64) and 30 (p. 65), is greater than comparative cases with the drier initial condition.

The simulation for the 10-cm deep source provided more preferable distribution of water than the other two source locations. The depletions that are shown in the lower half of the root zone, at the end of the drying cycles in Figures 19 (p. 53) and 20 (p. 54), are expected to be supplemented later from water near the source. Accumulation of water at the bottom even with the wetter initial condition and at the end of 44.0 hours of the drying cycle, Figure 28 (p. 63), is almost nil. This indicates that the distribution pattern is in close proportion to the actual consumption by the plant roots.

Considering the facts discussed above, it becomes evident that the 10-cm deep source provides better consumptive use and vertical distribution efficiency than the other two deeper locations of the source. This naturally leads one to make a general premise that the shallower the subirrigation source, the better the system. If the distribution of the consumption rate with depth, as assumed in Figure 5 (p. 17) is true, this is the expected conclusion. Thus, trickle irrigation may be considered to be the best irrigation system, if surface evaporation can be prevented effectively.

The simulation model, as presented in Table 2 (p. 19-22), was applied for irrigation from the surface. The initial water content was maintained at 0.32 (cm^3/cm^3) for this simulation. The resulting water content profiles at 12.0 and 21.0 hours during the irrigation cycle are shown in Figure 33. It is very interesting to note that the water content profile at the end of 21.0 hours remained very close to the initial profile, thus suggesting the possibility of a continuous irrigation for a very long time. Further simulation data in this area are necessary before making any definite conclusions. This solution is theoretically sound for a trickle irrigation system.

The simulation data obtained with initial uniform water content of 0.32 (cm^3/cm^3) were also analyzed in light of the availability coefficient, C_a, and the proportionality coefficient, C_p. These terms have been defined and discussed in section 4.2 of Chapter IV (p. 37 through 41). Since the desirable water content profile for a crop grown in Yolo light clay was not known, it was assumed to be a vertically uniform profile at the water content value of 0.32 (cm^3/cm^3). The end of the drying cycle was considered to be the most appropriate time for making measurements. For the purpose of comparison between the C_a and C_p values calculated from two distributions, it is necessary to have equal duration of the irrigation cycle.

In order to calculate the values of C_a and C_p, 25 points, the first one being at the surface, along the water content profiles were used for each case. The points selected were all 2.5 cm apart.

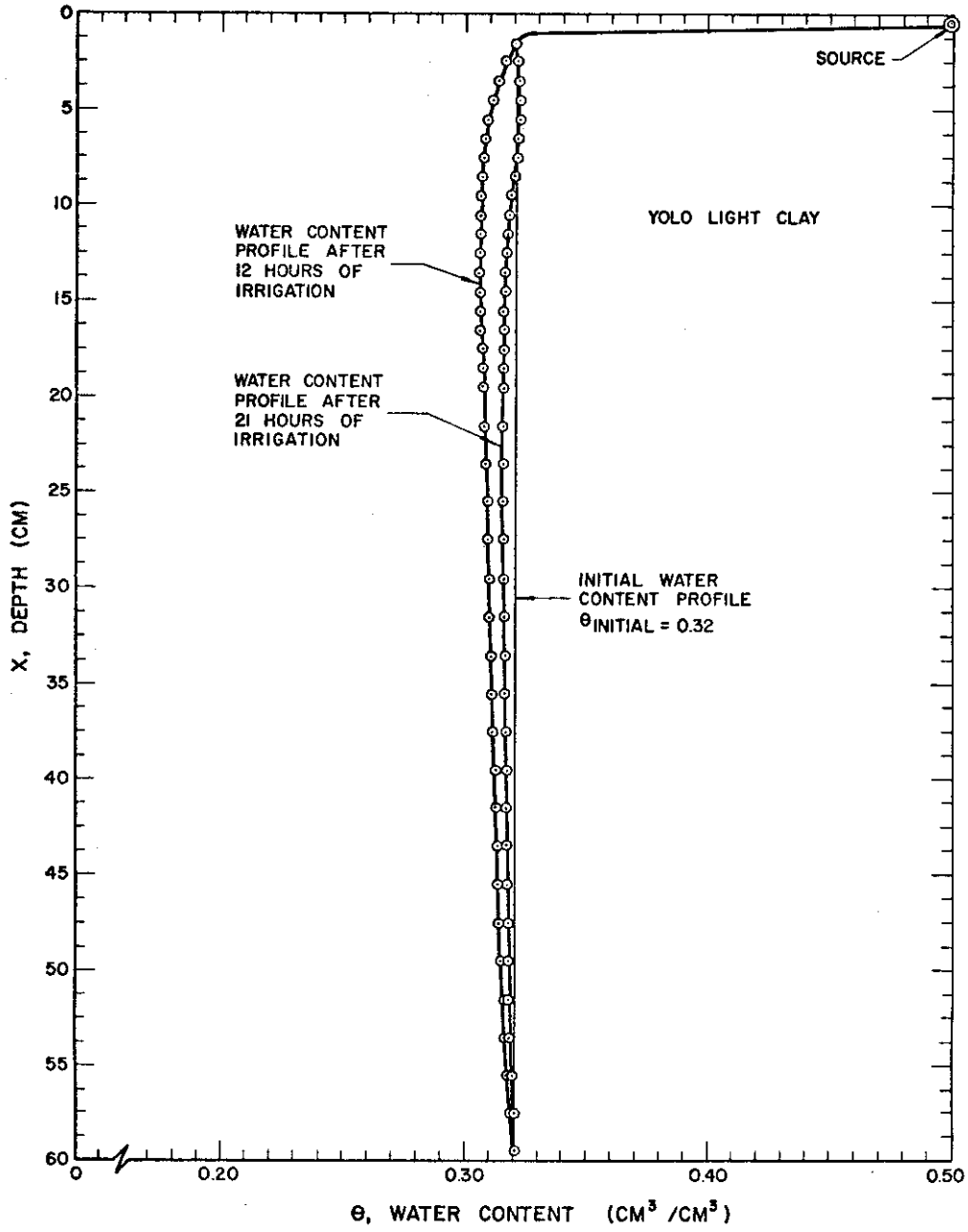

Figure 33 Water content profiles during infiltration from surface with initial uniform water content of 0.32 (cm^3/cm^3)

Table 7 shows the coefficient values with other pertinent information. Details of the calculation are given in Table 8.

Table 7 Calculated values of the availability coefficient, C_a, and the proportionality coefficient, C_p, from water-content profiles with initial uniform water content of 0.32 (cm^3/cm^3)

Item No.	Location (cm below surface) of Source	Control Points		Duration (hrs) of		C_a	C_p
		Irrigation cycle	Drying cycle	Irrigation cycle	Drying cycle		
1	10(Fig. 28)	2.5	9.5	10.43	44.00	.9254	.9234
2	20(Fig. 29)	12.5	19.5	4.15	57.18	.9468	.9468
3	20(Fig. 30)	8.5	19.5	13.00	115.00	.8920	.8915
4	30(Fig. 31)	22.5	29.5	4.15	78.00	.9256	.9240
5	30(Fig. 32)	18.5	29.5	12.73	165.04	.8783	.8774

Of the C_a and C_p values calculated for the 20- and 30-cm source solutions, items 2 and 4 of Table 7 are comparable because both of them have the same duration (4.15 hours) of the irrigation cycle. Both the C_a and the C_p values for the 20-cm source solution are higher than for the 30-cm one. In item 2, C_a and C_p have the same value because there was no point in the simulated profile at the end

Table 8 Calculation of the availability coefficient, C_a, and the proportionality coefficient, C_p, for solutions with initial uniform water content of 0.32 (cm^3/cm^3)

Point no.	Deviation of water content values (cm^3/cm^3) of the simulated profiles from the desirable value of 0.32 (cm^3/cm^3)				
	Fig. 28	Fig. 29	Fig. 30	Fig. 31	Fig. 32
1	-.008	.000	-.002	-.002	-.001
2	.004	.000	.000	-.002	-.002
3	.015	.002	.004	-.002	.004
4	.024	.007	.009	.002	.001
5	.032	.012	.014	.006	.004
6	.040	.017	.020	.010	.009
7	.058	.022	.024	.014	.013
8	.060	.027	.027	.018	.015
9	.061	.032	.030	.020	.018
10	.060	.034	.034	.023	.021
11	.050	.034	.038	.026	.024
12	.040	.034	.042	.028	.028
13	.034	.032	.046	.030	.031
14	.029	.030	.056	.033	.034
15	.025	.026	.058	.034	.038
16	.021	.023	.054	.034	.044
17	.016	.020	.046	.034	.058
18	.012	.018	.044	.035	.063
19	.008	.014	.044	.035	.067
20	.005	.012	.044	.036	.072
21	.003	.010	.044	.036	.076
22	.002	.008	.044	.036	.081
23	.002	.008	.044	.036	.086
24	.002	.008	.048	.037	.092
25	.002	.009	.052	.038	.098
$\sum \Delta x P_i$	.605	.427	.866	.601	.977
$\sum \Delta x n_i$	.008	.000	.002	.006	.003
$\sum \Delta x_i$	.613	.427	.868	.607	.980
N	25	25	25	25	25

Table 8 (continued)

	Fig. 28	Fig. 29	Fig. 30	Fig. 31	Fig. 32
$\frac{1}{N} \left\| \sum \frac{\Delta x P_i}{DW_i} - \frac{\Delta x n_i}{DW_i} \right\|$	.0746	.0532	.1080	.0744	.1217
$\frac{1}{N} \sum \frac{\Delta x_i}{DW_i}$	.0766	.0532	.1085	.0760	.1226
C_a	.9254	.9468	.8920	.9256	.8783
C_p	.9234	.9468	.8915	.9240	.8774

of the drying cycle with a water content value less than that of the desirable water content profile, as can be seen in Figure 29 (p. 64). Neglecting the difference between the irrigation cycle durations in, and comparing the values of the coefficients of, items 3 and 5 of Table 7 (p. 73), the 20-cm source solution is found to produce higher values of both C_a and C_p than the deeper source solution. The 10-cm source solution, item 1 of Table 7 (p. 73), has a much higher duration of the irrigation cycle (10.43 hours) compared to the duration (4.15 hours) for each of items 2 and 4. However, the values of C_a and C_p for item 1 are very nearly equal to those for item 4 and slightly less than those for item 2. From this, it is expected that with an irrigation cycle duration of 4.15 hours, the 10-cm source solution will yield much higher values of the coefficients than other solutions with the source at lower depths but having the same duration of the irrigation cycle.

The results from this analysis support the previous conclusion that the 10-cm deep source provides better efficiency than the other two deeper locations of the source. They also demonstrate the capacity of the coefficients, C_a and C_p, in measuring the effectiveness of vertical distribution of water in a subirrigation system. The accuracy of this analysis is, however, dependent on the validity of the assumed desirable water content profile with respect to actual field situations.

The computer model could be used to simulate data and determine irrigation schedules for each source location based on the soil-water

status alone. This, however, would require obtaining simulation results for several sequences of the irrigation and drying cycles in each case. It would be interesting to see if the systems attain a quasi steady-state situation over an extended period.

The questions of "when" and "how much" to irrigate can, however, only be answered through crop response measurements. In order to obtain a true measure of the plant water status, measurements should be made on the plant itself, not in the soil or the atmosphere. The status of the water in the plant represents an integrated effect of the atmospheric demand, soil-water potential, rooting density and distribution, as well as other plant characteristics. Clark and Hiler (1971) recommended leaf-water potential as a good measurement on plant for irrigation scheduling. It is expected that a dynamic computer model could be developed for irrigation scheduling which would consider the pertinent parameters involved.

It is known that in spite of enough water being available in the soil, plants wilt temporarily during certain critical periods of the day. This happens when the evapotranspirational demand for water exceeds the rate at which plant roots can extract water from the soil. Howell et al. (1971) established that by direct application of water by mist irrigation to the crop canopy during critical hours of the day, the plant-water balance was effectively controlled and the soil water utilization increased. A combination of mist and surface irrigation yielded as much as 60 percent more crops compared to the yields resulting from surface irrigation alone (Howell et al.,

1971). It is believed that a combination of subirrigation and mist irrigation would be a very desirable system. The present model could be adjusted to accommodate the necessary modifications for such a combined system. Two parameters, the leaf-water potential for the mist irrigation and the soil-water potential for the subirrigation, would have to be measured for irrigation scheduling. The entire system could be automated utilizing separate measuring devices located in the plant and in the soil.

The simulation results shown in this study are synchronized in time for the irrigation cycle to start at 6:00 a.m., as has been shown in Figures 3 (p. 15) and 4 (p. 16). The results will be different if the starting time is set at some other value. It may, however, be assumed that no appreciable difference in the simulation results will occur with a starting time of ± 2 hours from the assumed time.

In the model, the source has been incorporated by considering it to consist of a layer of saturated soil. This assumption is true when subirrigation is done by synthetic porous pipes which run just full so that the water at the outer periphery is at atmospheric pressure. Any pressure above atmospheric is not accounted for in the model, because the water content vs. pressure potential relationship, as shown in Figure 7 (p. 31), is not considered for any value of the pressure potential greater than zero. The apparent limitations of the applicability of the model are, however, not major. First, porous plastic pipes are available and are being used for

subirrigation. Second, it has been shown by Philip (1958) that the effect of positive pressure on the infiltration into unsaturated soils is negligible.

CHAPTER VI

SUMMARY AND CONCLUSIONS

A computer model was developed to simulate unsteady vertical flow of water in an unsaturated soil during infiltration from a buried source and through the following drying period. The model utilized S/360 CSMP (Continuous System Modeling Program), a recently developed language specially designed for digital simulation of transient phenomena that can be represented by differential equations. The model has the capacity to consider the source at any desired level. The effect of gravity and the consumption of water by plant roots which was considered to be a nonlinear function of the time of day were taken into account. The consumption rate at any given time was assumed to be distributed in a linearly decreasing manner with the depth of the root zone.

The principles of the conservation of mass and of Darcy's law, which lead to the derivation of the partial differential equation describing unsteady flow in unsaturated media, were applied directly in the development of this model. Its application required knowledge of the hydraulic characteristics of the chosen soil.

A particular form of the general model, which described the unsteady vertical infiltration through the surface, was applied to three different soils -- Yolo light clay, Adelanto loam, and Pachappa loam. In this particular solution consumption by plant roots was not

considered. The results for Yolo light clay compared favorably with the numerical solutions of Philip for the same soil and for identical boundary and initial conditions. The solutions for the other two soils demonstrated the workability of the model for soils having different hydraulic characteristics.

Two sets of simulation data for the general model were obtained for Yolo light clay using a soil depth as well as a root depth of 60 cm. The first set had an initial uniform water content of 0.2375 (cm^3/cm^3), whereas 0.32 (cm^3/cm^3) was the value for the second set. Boundary conditions always dictated a no-flow situation across the surface and an impermeable layer at the bottom of the soil mass. A daily total root consumption of 0.635 cm was used. In each set, three different depths of the source, i.e., 10, 20, and 30 cm, were used. For each source location, simulation results were obtained for varying durations of the irrigation and drying cycle. The length of time through which each cycle continued was controlled by a chosen water-content value at a specific point in the soil mass. The whole system, therefore, worked like an automated subirrigation installation.

The water-content profiles evaluated with time were plotted for each simulation run. The patterns of water distribution with time for each source location were analyzed in light of two important criteria: (i) adequacy of the supply of water with respect to the need at different parts of the root zone, and (ii) overall irrigation efficiency.

The S/360 CSMP language proved to be efficient in simulating the transient water flow phenomena in unsaturated soils. The principal advantage of the numerical procedure followed was in its complete generality and the ease with which numerical data on the hydraulic characteristics of the soil may be used without arbitrary assumptions and function fitting procedures. The model developed was not restricted to the boundary and initial conditions used for solutions in this study. Other conditions could be considered easily. Refinement of the present program also could accommodate other variables that may be deemed necessary.

As a result of this research, the following specific conclusions were drawn:

1. The unsteady vertical infiltration from the surface into an unsaturated soil was simulated accurately by the particular computer model developed in this work.

2. The general simulation model developed in this research can be used to describe the phenomena of transient vertical water flow in an unsaturated soil during infiltration from a buried source and redistribution through the following drying cycle, in a sequence, taking into account the root consumption activity. This model can conveniently be used to simulate water distribution phenomena involved in subirrigation practices.

3. Two new concepts are defined -- availability coefficient and proportionality coefficient. These help evaluate the effectiveness of vertical water distribution in a subirrigation system. The

water-use efficiency is the other area that needs to be considered for determining the overall efficiency of the system. Other segments of irrigation efficiency are generally very high in subirrigation by virtue of the nature of the application of water.

4. For the assumed distribution of the root consumption with time and depth, the 10-cm depth source provided better distribution of water with time and space compared to the 20-cm and 30-cm source locations. Irrigation from zero depth, as in the case of trickle irrigation, appeared to be the best system for the given boundary and initial conditions.

REFERENCES

1 Bhuiyan, S. I., E. A. Hiler, C. H. M. van Bavel, and A. R. Aston. 1971. Dynamic simulation of vertical infiltration into unsaturated soils. Water Resources Research (in press).

2 Clark, R. N. and E. A. Hiler. 1971. Plant measurements as indicators of moisture stress in crops. Annual Meeting of the ASAE. Paper No. 71-231. 25p.

3 Curry, R. B. Dynamic modeling of plant growth. 1969. Winter Meeting of the ASAE. Paper No. 69-939. 17p.

4 Danielson, R. E. 1967. Root systems in relation to irrigation, p. 390-424. In: Hagan et al., (ed.) Irrigation of agricultural lands. American Society of Agronomy. Madison, Wisconsin.

5 De Backer, L. W. and L. Boersma. 1968. Le facteur d'exploration radiculaire: un nouveau concept dans l'etude de l'utilisation de l'eau du sol par les plantes. Supplement au Bulletin de l'Association Francaise pour l'Etude du sol. Science du Sol -- No. 2:3-20.

6 De Wit, C. T., R. Brouwer, and F. W. T. Penning de Vries. 1970. The simulation of photosynthetic systems. In: Prediction and measurement of photosynthetic productivity. International Biological Program Primary Production. 1969 Trebon Meeting. Center for Agricultural Publishing and Documentation. Wageningen. 632p.

7 Gardner, W. R. 1962. Approximate solution of a non-steady-state drainage problem. Soil Sci. Soc. Amer. Proc. 26(2):129-132.

8 Hall, N. S., W. F. Chandler, C. H. M. van Bavel, P. H. Reid, and J. H. Anderson. 1953. A tracer technique to measure growth and activity of plant root systems. North Carolina Agr. Exp. Sta. Tech. Bull. 101. 40p.

9 Hammes, J. K. and J. F. Bartz. 1963. Root distribution and development of vegetable crops as measured by radioactive phosphorous injection technique. Agron J. 55(4):329-333.

10 Howell, T. A., E. A. Hiler, and C. H. M. van Bavel. 1971. Crop response to mist irrigation. Annual Meeting of the ASAE. Paper No. 71-203. 23p.

11 IBM Corporation. 1967. System/360 continuous system modeling program (360-A-CX-16X). User's manual. Data Processing Division. 112 East Post Road. White Plains, N. Y. 61p.

12 Israelsen, O. W. and V. E. Hansen. 1965. Irrigation principles and practices. John Wiley and Sons, Inc. New York. 447p.

13 Jackson, R. D., R. J. Reginato, and C. H. M. van Bavel. 1965. Comparison of measured and calculated hydraulic conductivities of unsaturated soils. Water Resources Research 1(3):375-380.

14 Klute, A. 1951. Some theoretical aspects of the flow of water in unsaturated soils. Soil Sci. Soc. Amer. Proc. 16(2):144-148.

15 Lambert, J. R. 1971. The use of CSMP for agricultural engineering problems. Annual Meeting of the ASAE. Paper No. 71-529. Pullman, Washington. 38p.

16 Moore, R. E. 1939. Water conduction from shallow water tables. Hilgardia 12(6):383-426.

17 Nakayama, F. S. and C. H. M. van Bavel. 1963. Root activity distribution patterns of sorghum and soil moisture conditions. Agronomy J. 55(3):271-274.

18 Nielsen, R. D., D. Kirkham, and W. R. van Wijk. 1961. Diffusion equation calculations of field soil water infiltration profiles. Soil Sci. Soc. Amer. Proc. 25(3):165-168.

19 Philip, J. R. 1957a. The theory of infiltration:1. The infiltration equation and its solution. Soil Sci. 83(5):345-357.

20 Philip, J. R. 1957b. The theory of infiltration:5. The influence of initial moisture content. Soil Sci. 84(4):329-339.

21 Philip, J. R. 1958. The theory of infiltration:6. Effect of water depth over soil. Soil Sci. 85(5):278-286.

22 Philip, J. R. 1968. Comments on the paper by R. Singh and J. B. Franzini, "Unsteady flow in unsaturated soil-water movement from a cylindrical source." J. Geophys. Res. 73(12):3968-3971.

23 Philip, J. R. 1969. Theory of infiltration, p.215-296. In: Ven T. Chow, (ed.) Advances in Hydroscience. Vol.5. Academic Press. New York.

24 Shih, S. and G. J. Kriz. 1969. Transient radial flow in unsaturated soil. 50th Annual Meeting. Amer. Geophys. Un. Paper No. H-87. Washington, D. C. 18p.

25 Singh, R. 1970. Flow from a spherical source with water content dependent diffusivity. Water Resources Research 6(4):1140-1147.

26 Singh, R. and J. B. Franzini. 1967. Unsteady flow in unsaturated soils from a cylindrical source of finite radius. J. Geophys. Res. 72(4):1207-1215.

27 Wang, F. C. 1963. An approach to the solution of unsteady unsaturated flow problems in soils. Department of Civil Engineering Technical Report No. 19. Stanford University. 105p.

28 Wierenga, P. J. and C. T. de Wit. 1970. Simulation of heat transfer in soils. Soil Sci. Soc. Amer. Proc. 34(6):845-848.

29 Whisler, F. D. and A. Klute. 1965. The numerical analysis of infiltration, considering hysteresis into a vertical soil column at equilibrium under gravity. Soil Sci. Soc. Amer. Proc. 29(5):489-494.

30 Whisler, F. D., A. Klute, and R. J. Millington. 1968. Analysis of steady-state evapotranspiration from a soil column. Soil Sci. Soc. Amer. Proc. 32(2):167-174.

31 Whisler, F. D. and K. K. Watson. 1968. One-dimensional gravity drainage of uniform columns of porous materials. Journal of Hydrology 6(3):277-296.

32 Zetzsche, J. B. and J. S. Newman. 1966. Subirrigation with plastic pipe. Agricultural Engineering 47(2):74-75.

LIST OF SYMBOLS AND ABBREVIATIONS

δ	partial derivative
ρ	fluid density
θ	water content
t	time
v	volume flux
x, y, z	axes of the coordinate system
Δx, Δy, Δz	small change in the x, y, and z direction, respectively
K	hydraulic conductivity
ϕ	hydraulic potential
$\nabla\cdot$	divergence of
∇	gradient of
h	pressure potential
X, x	vertical ordinate
ν, χ, ψ, ... $f_m(\theta)$	coefficients which are functions of θ in equation (7)
S	source term
C_a	availability coefficient
C_p	proportionality coefficient
N	number of observations
$\Delta x P_i$	positive value of the deviation of water content of ith observation from the desired water content of that point

LIST OF SYMBOLS AND ABBREVIATIONS (continued)

Δxn_i	negative value of the deviation of water content of ith observation from the desired water content of that point
DW_i	desired water content of ith observation
Δx_i	absolute deviation of water content of ith observation from the desired water content at that point
$\sum$	summation
CSMP	continuous system modeling program
S/360	system/360
NL	number of layers
IPIPE	layer number of the source
TX	thickness of layer
DX	distance between centers of two adjacent layers
X, x	gravitational potential
PRPOT	pressure potential
HYDPOT	hydraulic potential
COND	hydraulic conductivity
KOND	average hydraulic conductivity across the top boundary of a given layer
ICON	initial water content
WCON	water content
FLOWIN	rate of flow across the top boundary of a given layer

LIST OF SYMBOLS AND ABBREVIATIONS (continued)

NFR	net rate of flow
INRATE	rate of infiltration
TOTINT	total amount of infiltration
RTCON	root consumption rate of a given layer
RFACT	root factor
UPTAKE	root uptake rate
RTIME	time of day
WCONT	function giving pressure potential vs. water content relationship
CONDT	function giving water content vs. hydraulic conductivity relationship
POT	function giving water content vs. pressure potential relationship
RDISTN	function giving depth vs. root factor relationship
CONSUM	function giving time of day vs. uptake rate relationship
$Y_{t+\Delta t}$	value of y at time $t+\Delta t$
Y_S	value of $Y_{t+\Delta t}$ calculated by Simpson's Rule
A	absolute error
R	relative error
CM, cm	centimeter or centimeters
HRS, hrs	hours
SEC	second or seconds

LIST OF SYMBOLS AND ABBREVIATIONS (continued)

p.	page
Fig.	figure
CDT	central daylight time